Chapter 1 Introduction

1.1 Introduction

Te-Chi Reservoir is the main water source for the Taichung metropolitan area. Since this reservoir receives sufficient water resources and is far from the artificial pollutants, therefore it is the best drinking water source of Central Taiwan for decades. Recently, because of the heavily developing of high mountain agriculture with a large amount applied pesticides and fertilizers which had been carried into the reservoir by either water of storm or mudslide. Those organic fertilizers cause the heavy eutrophication and then generate the abundance of nature organic matters (NOMs) into the lake.

NOMs are composed of a complicated mixture of organic compounds, which can be of human origin or the result of natural degradation processes causes many water quality problems, e.g. odor, taste and color.

Ozone is an effective oxidation agent and able to decompose various organic and inorganic substances in water. It is usually used in water treatment as an intermediate disinfectant, an effective oxidant and as an agent of the decolornization of treated water. But it is also known to be

an unstable compound with low solubility in aqueous solution and low reactivity toward to some inactive aromatic compounds during ozone reactions. Therefore, it is very important to improve the ozone oxidation capability for effectively decomposing the complicated substances. In order to improve the efficiency of ozonation, new methods of advanced oxidation processes (AOPs) were proposed to provide the effective methods for removing the contaminants from water treatment process. The increase in efficiency is also implying from an economic point of view because of the ozone generation is still considered to be a relatively expensive process. Under the typical drinking water treatment practice, the total organic carbon concentration can not be reduced by using the ozonation alone. However, it only makes the NOMs' structural changes.

Heterogeneous catalytic ozonation is a novel type of AOPs that combines ozone with the adsorptive-oxidation properties of solid phase oxide catalysts to achieve mineralization of some dissolved organics in water. The main advantage of supported catalyst is the separation of the solid catalysts from liquid phase and increase ozone capability for the reduction of refractory organic pollutants. The catalyst,

perfluorooctylalumina (PFOA) (Kasprzyk-Hordern and Nawrocki, 2003), can increase the efficiency of ozonation system by adsorbing the ozone molecules to improve the dissolution and stability of ozone in water, resulting in high degradation rates of organic contaminants. However, due to the difficulty of recovery the powder form of PFOA, using a magnetic carried coated method to assembly magnetic PFOA (MPFOA) particles had been applied for recycling propose.

Magnetic drug delivery and separation technologies have been attractive in the field of biology and medicine, due to their great advantage, such as effective control, high speed, accuracy, and simplicity in compares with the conventional separation. Combining with the use of novel magnetic separation process, the magnetic particle technology has a high potential to be applied in the adsorption systems. In order to remove the target pollutants or compounds from water, the magnetic particles can be modified by the combination or modification of functional groups or inorganic compounds and yielding the magnetic adsorbents. Both the particle recovering and the ozonation efficiency have been significantly improved by this coating method. The investigation of the characteristics of the novel catalysts were carried out

by using the scanning electron microscopy with energy dispersive spectrometer (SEM/EDS), superconducting quantum interference device (SQUID) and X-ray powder diffraction (XRD). On-line measurement of oxidation reduction potential (ORP) was adapted as an indicator to measure the difference between the uncatalyzed and catalyzed ozone systems for comparison. The change of functional groups during ozonation and ozonation with MPFOA were examined by Fourier-transform infrared spectrophotometer (FTIR) and ^{13}C nuclear magnetic resonance (^{13}C NMR) spectra. A modified Nernst equation model, established based on the measured data, can be used to predict the overall reactions. The synthesized magnetic catalyst for recycling purpose can provide the upgrade ozonation technique in the water treatment technique.

1.2 Objectives

The objectives of this study are:

1. Comparing the basic water quality, the composition of NOMs of Te-Chi Reservoir
2. Synthesizing the MPFOA catalyst
3. Applying catalyst to enhance the efficiency of ozonation
4. Establishing a Nernst type model to the MPFOA-O_3 system
5. Applying FTIR and ^{13}C NMR to investigate the change of the functional groups during ozonation

Chapter 2 Literature review

2.1 Natural organic matters in reservoir

Natural organic matters (NOMs) are composed by many complex substances and shown as a heterogeneous mixture organic compound. NOMs can be broadly divided into two fractions: humic substances (HS), which are composed of fulvic, humic acids and non-humic substances (non-HS), which include carbohydrates, lipids, and amino acids (Karnik *et al.*, 2005). Te-Chi Reservoir, water supplies for the Taichung metropolitan area, central Taiwan, ROC, which is sufferings of the excess agricultural discharge containing pesticides and fertilizers from the upstream and caused eutrophication problems. The eutrophicated water contains substantial amount of the complex organic matters, which could cause serious water quality problems, i.e., odor, color and taste.

Leenheer (1981) had proposed a comprehensive method for the NOMs isolation-fractionation approach. By this procedure, NOMs can be extracted and separated as the components of fulvic acid, humic acid, hydrophilic acids, hydrophobic neutrals, hydrophilic neutrals, hydrophobic bases and hydrophilic bases. The factions are eluted by using the water in series through columns containing XAD-8 resins.

The mechanisms of the ozonation for NOMs in water are still not well understood because of the wide diversity of NOMs with very different chemical properties. There is a need to better understand the effect which different NOMs' characteristics have on the decomposition by ozone. An appropriate selection of the reaction conditions is necessary to upgrade the ozonation efficiencies.

2.2 Application of ozone

2.2.1 Advanced oxidation processes (AOPs)

AOPs are widely used in the water treatment technologies for organic pollutants which can not be removed con degraded by conventional techniques because of their high chemical stability and low biodegradability (Malato *et al.*, 2007). Schrank *et al.* (2007) pointed out that AOPs predominantly involve the generation of very powerful and non-selective oxidizing species, i.e. hydroxyl radicals (•OH), for the destruction of refractory and hazardous pollutants observed in industrial wastewaters, surface waters and groundwater.

Ozonation has been demonstrated to be an effective oxidation technology for the decomposition of certain micropollutants in water.

Ozone can either react directly with organic compounds, or decompose to •OH, which also reacts with the target compounds (von Gunten, 2003). The vigorous treatment results in the complete oxidation or mineralization of NOMs to CO_2 and reduces the total organic carbon (TOC) content. It also partially oxidizes NOMs and cleaves the large molecular weight constituents into smaller and more biodegradable compounds such as aldehydes and carboxylic acids (Toor and Mohseni, 2007; Alsheyab and Muñoz, 2007).

2.2.2 Two-stage ozone reactions

The reaction of ozone with organic substrates follows two reaction mechanisms: (1) the molecular ozone oxidation (direct reaction), and (2) the free radical oxidation (indirect reaction) (Hoigné and Bader, 1976).

Ozone molecular direct oxidation:

Ozone selectively attacks the unsaturated electron-rich bonds and easily reacts with specific functional groups, such as aromatics, olefins and amines (Hoigné and Bader, 1983). In general, the reaction by direct ozone reaction is slower than that of hydroxyl radical reaction.

Hydroxyl radicals indirect oxidation:

The indirect reaction of hydroxyl radicals is generated by the decomposition of ozone molecule, while the hydroxyl radicals' reaction rate is fast and the selectivity is low (Prado *et al.*, 1994). In water, ozone may react directly with dissolved substances, or it may decompose to form secondary oxidants, hydroxyl radicals, which are extremely powerful and non-specific oxidants that react with many organic and some inorganic species (Pi *et al.*, 2005).

Direct ozonation involves the degradation of organics by ozone molecule under acidic conditions, while the term indirect ozonation consider the degradation mechanisms of organics throughout hydroxyl radicals and it occurs under basic conditions (Chu *et al.*, 2006). In direct mechanism, the hydrogen peroxide participates in redox reactions where it can behave as an oxidant or as a reductant, while indirect mechanism consider formation of free radicals throughout the reactions by other inorganic compounds, such as ferrous ions, or by photolysis. In the direct mechanisms, the oxidants ozone and hydrogen peroxide have much lower standard redox potential, 2.07 and 1.77 V, respectively, than 2.80 V of •OH, species formed the by indirect mechanisms of above oxidants. The determination of reaction rates and the prediction of the ozonation

performance for the cases of direct oxidation by ozone molecules and indirect oxidation by •OH have been proposed.

2.2.3 Hydroxyl radicals measurement

Monteagudo *et al.* (2005) reported that ozone reaction is known to produce the secondary oxidants, such as the OH radicals, a much more powerful oxidant than ozone, to oxidize a wide range of organic compounds with non-selectively. Meunier *et al.* (2006) also reported that OH radicals is one of the most reactive species in ozonation and the amount of OH radicals seems to correlate with rate of the decomposition of ozone. However, there are very little papers dealing with the study of concentration and the dynamics of OH radicals. Therefore, the measurement of OH radicals is important for investigating the ozonation mechanisms. Sánchez-Polo *et al.* (2005) indicated that due to the high reactivity of OH radicals toward to organic substances, hence, the presence of OH radicals concentrations are too low to be quantified. HPLC is widely utilized because of its sensitivity and selectivity, and its analysis technique has been developed to indirect detect unstable radicals recently. Louit *et al.* (2005) proposed the method allowing

identification form the reaction of the products of coumarin and ozone under various conditions; wherever possible these products have been quantified. This study adapts the proposed analysis method to investigate the free radical in ozone and ozone with catalyst mechanisms.

2.2.4 The catalytic ozonation

Heterogeneous catalysis is a novel method in AOPs while catalytic ozonation may become a new tool of water treatment. Many articles mentioned the application of various catalysts coupled with ozone in order to enhance the treatment efficiency and decompose different organic compounds from water. Catalysts such as MnO_2 (Ma *et al.*, 2005), titanium dioxides or alumina-supported catalysts such as TiO_2/Al_2O_3, Fe_2O_3/Al_2O_3 (Kasprzyk-Hordern *et al.*, 2003; Beltrán *et al.*, 2005), and many other catalysts were proposed to enhance the efficiency of ozone reaction with organic matters. Various catalysts were identified to improve the oxidation of certain organic compounds in the presence of dissolved ozone in treated water (Ni *et al.*, 2003; Qu *et al.*, 2004).

Kasprzyk-Hordern *et al.* (2004) reported a high efficiency of HAs and NOMs removal from water due to ozonation in the presence of

perfluorooctylalumina (PFOA) and therefore enhancing its stability and solubility in water, resulting in high degradation rate of organic contaminants present in water.

2.3 Magnetic technology

2.3.1 Magnetic particles and magnetic separation

National Aeronautics and Space Administration (NASA) scientist, Papell (1965) developed the production of the magnetic fluids in 1965. Thereafter, the magnetic drug delivery and separation technologies have been attractive in the fields of biology and medicine, due to their great advantages; they are more effective control, high speed, accuracy and simplicity than the conventional separation (Rudge *et al.*, 2000; Peng *et al.*, 2004). Theoretically, an ideal magnetic separation must have superparamagnetism, chemical stability and uniform size. Magnetic separation is relatively rapid, cost effective and highly efficient than other processes. It has been widely used in various fields of biotechnology and biomedicine, such as cell separation, enzyme immobilization, protein separation, nucleic acid purification and immunoassay (Nitin *et al.*, 2004).

2.3.2 Magnetic application

Magnetic nanoparticles of iron oxides have many important applications in the fields of biotechnology and biomedicine. Most of these applications require the magnetic nanoparticles to be chemically stable, uniform in size and well-dispersed in liquid media.

1. Chemical coprecipitation method (Shen *et al.*, 1999):

Magnetic nanoparticles make up various nanostructured materials, such as magnetite, maghemite, nickel and cobalt. Among superparamagnetic magnetite (Fe_3O_4) nanoparticles, it makes a facile and cheap method which has been widely be used.

Nanoparticles Fe_3O_4 can be synthesized by a chemical coprecipitation method. The preparation procedure is performed with the presence of a high Fe (II) salt concentration without Fe (III) derivatives induce the formation of micrometer Fe_3O_4 particles.

2. Stöber method (Stöber and Fink, 1968):

Silica was coated on the surface of magnetite nanoparticles to form the superparamagnetic silica nanoparticles by a sol-gel method (Ma *et al.*, 2006). The nanoparticles are well dispersed without aggregation indicating the stabilization function of silica coating to the magnetic

Fe_3O_4 nanoparticles. Silica coating stabilizes the magnetite nanoparticles in two different ways. One is sheltering the magnetic dipole interaction through the silica shell. The other one is bringing the negative charge on the surface of silica shells, which enhances the coulomb repulsion of the magnetic nanoparticles. Thus the magnetic dipole interactions among the magnetic nanoparticles were greatly screened and they could be well dispersed. The surface of Fe_3O_4 has a strong affinity toward silica; no primer was required to promote the deposition and adhesion of silica (Philipse *et al.*, 1994). Silica was formed in situ through the hydrolysis and condensed of a sol-gel precursor, such as tetraethyl orthosilicate (TEOS) and subsequent condensation of silica onto the surface of Fe_3O_4 cores (Lu *et al.*, 2002).

Magnetic silica nanospheres with metal have the advantage in the segregation under the influence of external magnetic field and have the flexibility of charging various metal ions for specific separation system (Ma *et al.*, 2006).

2.4 Modeling

Variations of the system ORP of an oxidation-reduction process

caused by electron transfer can be delineated by the Nernst equation and expressed as (Weber, 1972).

$$E = E^0 + (RT/nF)\ln([Oxi]/[\mathrm{Re}\,d]) \quad \text{(Eq.1)}$$

The oxidation-reduction reaction is known to taken place by an electron transfer from substrate to oxidant. The use of ORP for the system to control the AOP process and apply model to simulate the reaction has been proposed by many researchers (Chang *et al.*, 2004; Liao *et al.*, 2007). Theoretically, a modified Nernst equation model, established based on the measured data, can predict the overall redox reaction.

2.5 Change of functional groups

Fourier transform spectrophotometer (FTIR) and CPMAS Carbon-13 nuclear magnetic resonance spectrums (^{13}C NMR) have been preciously applied for both quantitative and qualitative characterizations of NOMs (Wiles *et al.*, 2007). The method by measuring the spectrum of NOMs using FTIR and ^{13}C NMR spectrometers has been acknowledged as the adequate processes to estimate the humic properties.

FTIR has been widely used for the micro structural investigation.

When the samples are exposed to the infrared radiation, the samples will absorb the radiation which is corresponding to the vibrational energy of covalent bonds. The resulting absorption wavenumber are the unique fingerprint of compound. FTIR analysis allows the identification of inorganic and organic functional groups.

Kim and Yu (2005) applied FTIR to study the functional groups of NOMs in the raw water from Han River water, Korea. Kanokkantapong *et al.* (2006) found that the FTIR analysis of the isolated samples informs about the distribution of functional groups within the organic fractions and provides a basis for the comparison of compositional differences between the isolate a components from Bangkhen Water Treatment Plant, Thailand.

^{13}C NMR is a very useful tool in determining the types of carbons of NOMs. Spectrum can be obtained from a diluted liquid or a solid sample and the chemical shifts of the spectral peaks are assigned acceding to the different chemical environments (Koshino *et al.*, 2006; Satoh *et al.*, 2005). Park and Yoon (2007) carried out the ^{13}C NMR analysis of the hydrophobic and hydrophilic fraction of HA after the separation using XAD-8 resins.

In our best acknowledge, up to data, only too small amount literatures to well investigate the mechanisms of ozonation with catalyst. Therefore, we attempt to investigate the ozonation state with catalyst for the eutrophic Te-Chi Reservoir water in this study. Moreover, ^{13}C NMR and FTIR will be applied to investigate the relationship between the variations of functional groups characteristic of nature organic matter and the ozonation condition to determine, and then the feasibility of ozonation with the presence of the catalyst.

Chapter 3 Material and Methods

3.1 Experimental

The sampling site was at the upstream of Te-Chi Reservoir, where during the some seasons, the pollutant containing pesticides and fertilizer from agricultural farm could be injected to Te-Chi Reservoir to cause the eutrophication. The objective of this study is to investigate the raw water quality and the extracted components of nature organic matters (NOMs). This study also attempts to investigate the mechanisms of ozonation with and without catalyst of the Te-Chi Reservoir raw water.

Experimental flow chart for ozonation in the study is shown in Figure 3.1. The experimental processes include:

(1) Sample preparation and analysis: the water sample was collected from Te-Chi Reservoir and was analyzed on site to obtain of basic water quality (pH, TDS, DO, ORP, temperature and conductivity). Then the water sample was filtered by a 0.45 μm cellulose acetate glass filter in the laboratory and proceeded with the following basic analysis items. The analyzed items include COD, DOC, hardness, alkalinity and NH_3-N.

(2) Isolation and fractionation: The extraction procedures utilized in the

study were following the procedures described by Thurman and Malcolm (1981) and Leenheer (1981). Amberlite XAD-8 (Amberlite XAD, Sigma, USA) was packed in Pyrex glass columns for isolating the five categories of organic fractions such as HA, FAs, hydrophobic bases, hydrophobic neutrals and hydrophilic fractions from Te-Chi Reservoir raw water.

(3) Ozonation with/without presently catalyst: Te-Chi Reservoir raw water and the extracted HAs were ozonation with/without presence of catalyst; both of processes were monitored by an on-line oscilloscope measurement system. The on-line monitored data of pH, ORP, DO_3 and absorbance at the wavelength of 254 nm (A_{254}) were used to investigate the processes on the ozonation. The characteristics of catalytic MPFOA were determined by using the SEM/EDS, SQUID and XRD. The collected water samples were frozen and dried first, then analyzed by FTIR and ^{13}C NMR.

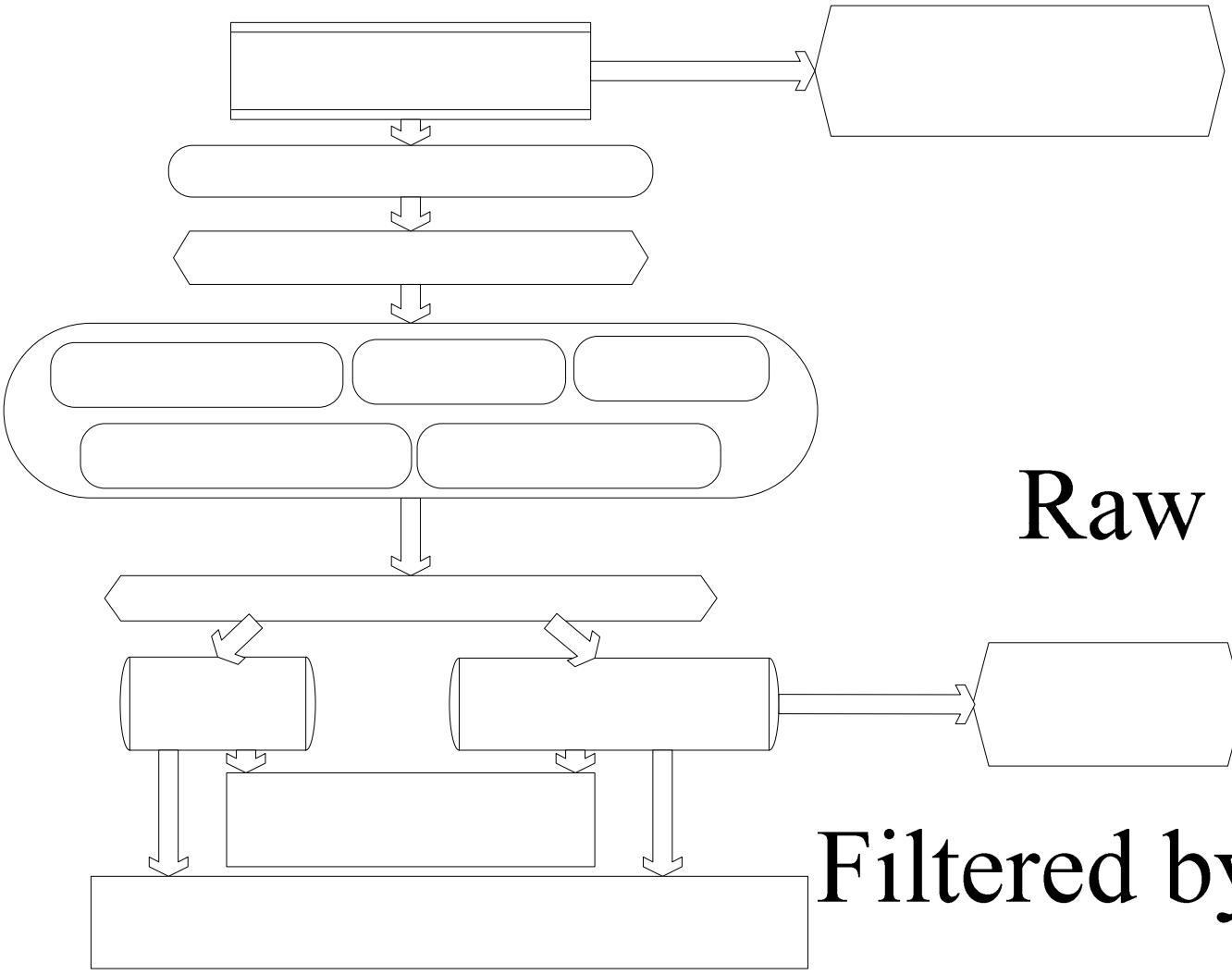

Figure 3.1 The experimental design and analysis process of this study.

Extracted b

Hydrophobic bases

Hydrophilic fraction

3.2 Methods and Instruments

3.2.1 Sampling site

The sample for study was collected from Te-Chi Reservoir at Taichung County, Taiwan on August 24, 2006. Polyethylene buckets contained 20 L of water samples mere covered by black plastic bag to prevent the effect of photolysis on the change of raw water. The water sample was preserved at 4 ℃ before analysis. Sampling location is shown in Figure 3.2 and the items which analyzed on site including: pH, ORP, DO, TDS, water temperature and conductivity.

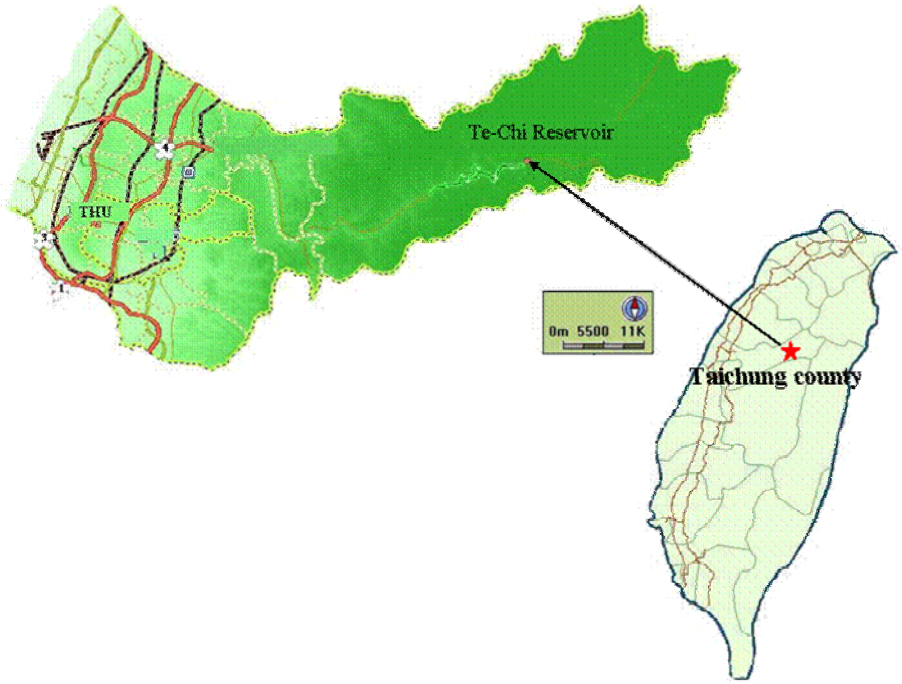

Figure 3.2 The water sampling location of Te-Chi Reservoir, which supply water for domestic water in Tai-Chung area, central Taiwan, ROC.

Figure source: PaPaGO software

3.2.2 Extraction procedure

The pre-treatment of XAD-8 resins:

(1) Resins cleaned by methanol, then soaked in 0.1 N NaOH solutions for 72 h followed by pure water washing step.

(2) Resins were settled in a Soxhlet extractor and washed with methanol, hexane, acetonitrile and methanol, respectively for 24 h.

(3) The resins were rinsed finally with pure water several times to remove the residual methanol, and then packed in Pyrex glass columns (5 cm internal diameter and 60 cm length).

(4) Aqueous NaOH (0.1 N, 1 L) and aqueous HCl (0.1 N, 1 L) (flow rate: 25mL min^{-1}) were alterative passed through the resins in the glass tube, and repeated twice. To make sure the XAD-8 resins free from methanol, the rinsed water effluent was examined by TOC. The resins cleaning procedure with pure water were repeated until the TOC concentration in the effluent was below the detection limit of 0.02 mg L^{-1}.

The separation procedure used in this study was described by Thurman and Malcolm (1981) and Leenheer (1981). The organic components were extracted from raw water and classified into humic

acids, fulvic acids, hydrophobic neutrals, hydrophobic bases and hydrophilic fractions by amberlite XAD-8 (Amberlite XAD, Sigma, USA) as absorbent for the separation NOMs in this study.

The reagents and equipments for the separation process are shown in Table 3.1. The fractionation procedures of organic matters from Te-Chi Reservoir raw water are shown in Figure 3.3. First of all, to remove the suspended solids, a 100 L water sample was filtered through a 0.45 μm cellulose acetate filter paper and the pH of sample was adjusted to 7 by adding HCl. Secondly, the filtered water was passed through the first XAD-8 resins column at a flow rate of 25 mL min^{-1} and then eluted with 0.1 N HCl for recovering the hydrophobic bases, which adsorbed on the resins. The pH of effluent from the first XAD-8 resins column was adjusted to 2 with 2 N HCl. The brown solution was introduced in to the second XAD-8 resins column under the flow rate of 25 mL min^{-1}. The NOMs contained in the filtrate from the second XAD-8 resins column was collected as the hydrophilic fractions. The NOMs absorbed onto the second XAD-8 resins was eluting by 0.1 N NaOH, which obtained the brown solution and the pH was adjusted to 1 with 0.1 N HCl. After that, it was passed through a 0.45 μm glass membrane

filter. The filtrate contained FAs and HAs were left on the filter membrane. The HAs was removed from filter by dissolving in 0.1 N NaOH and preserving in polyethylene bottles. The remaining fraction in XAD-8 resins in the second column was packed into filter tube, dried at 60 ^{o}C and washed with methanol to collect hydrophobic neutrals. A vacuum apparatus combined with high-purity nitrogen gas (99.99 %) was used to evaporate the methanol solution. The concentrated hydrophobic neutrals were redissolved in deionized water as a stock solution.

Table 3.1 Summary of the reagents and equipments for NOMs water separation from Te-Chi Reservoir by resin extraction process

Equipment	Series Number, Maker, Country
Glass column	Pyrex 5 cm, ID×60 cm, local supply
Teflon tubing	Reorder#06409-14, USA
Peristaltis pump	Peristaltic pump System Model No. 7553-80, Cole-Parmer, USA
Soxhlet extractions	Pyrex, local supply
Reagent (GR)	Catalog Number, Country, Country
XAD-8 resin	Amberlite XAD-8, Sigma, USA

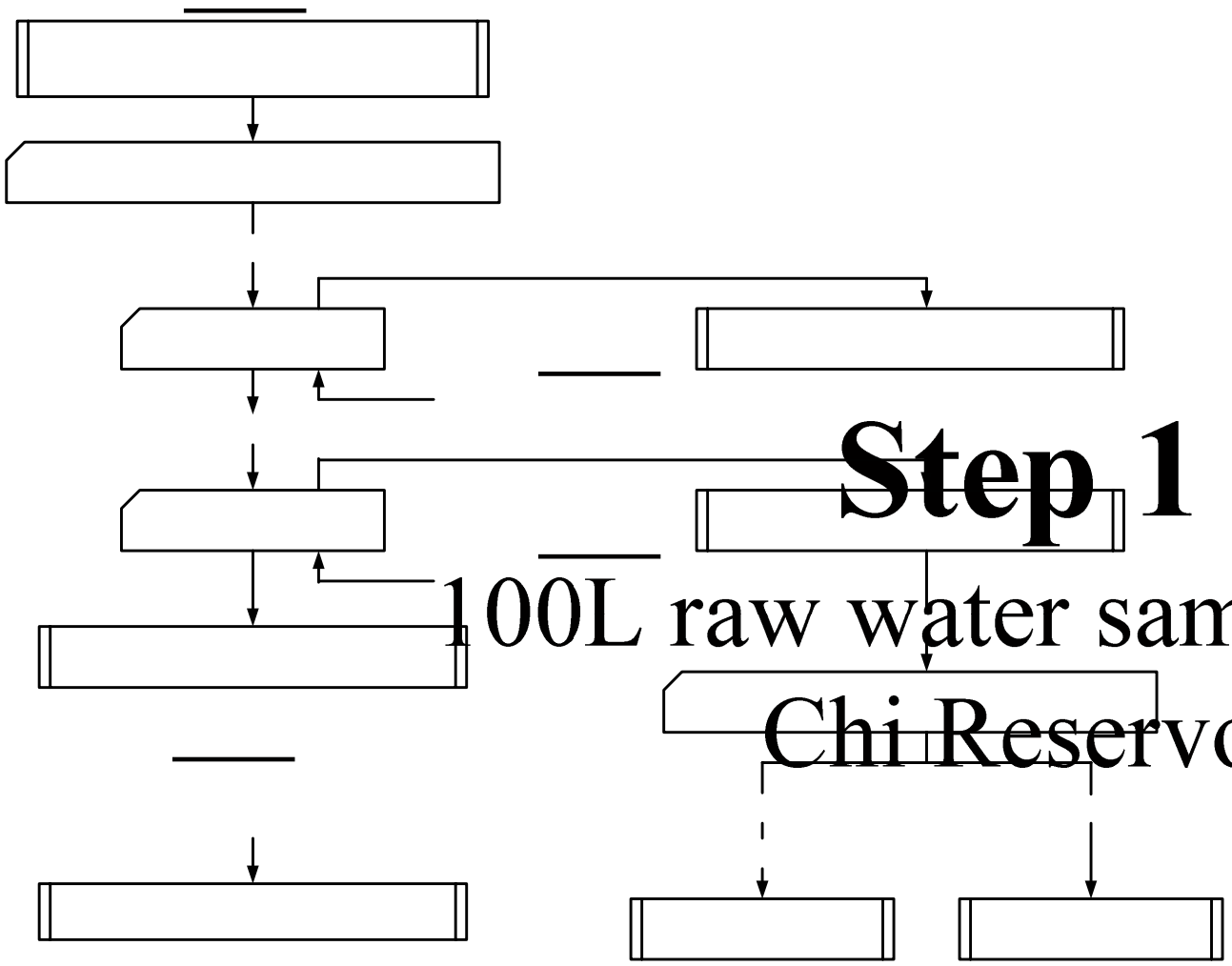

Figure 3.3 The flowchart for separation of five NOMs categories (HAs, FAs, hydrophobic bases, hydrophobic neutrals and hydrophilic fractions) from Te-Chi Reservoir raw water by separation process from XAD-8 resins.

Adjust pH to 7 with

XAD-8 Resins

Adjust pH to 2 with 2N

3.2.3 Ozonation system

The batch ozonation experimental system in this study is shown in Figure 3.4. The reactor (5 L) is equipped with a mixer rotating at 275 rpm. The temperature was maintained at 25 ± 2 ^{o}C by submerging the reactor into a water bath. Ozone is produced by an ozone generator (KA-1600, AirSep Corp., USA) and continuously introduce into the reactor at a flow rate of 10.53 g/hr. The maximum practical ozone concentration in deionizer distilled water is found to be 2.5 mg/L at 25 ± 2 ^{o}C by an on-line ozone analyzer. To obtain the instantaneous experimental data during the reaction, two on-line monitoring sensors (ORP, Mettler, Switzerland and pH, Mettler, Switzerland), oscilloscope (Yokogawa, OR100E, Japan), absorbance sensor are also inserted in the reactor. The optical fiber probe connected to an on-line UV detector and spectrophotometer (Cary-50, Australia) was injected into the reactor for monitoring the rapidly changing data. The Cary Win UV software is used to acquisite the monitoring conditions.

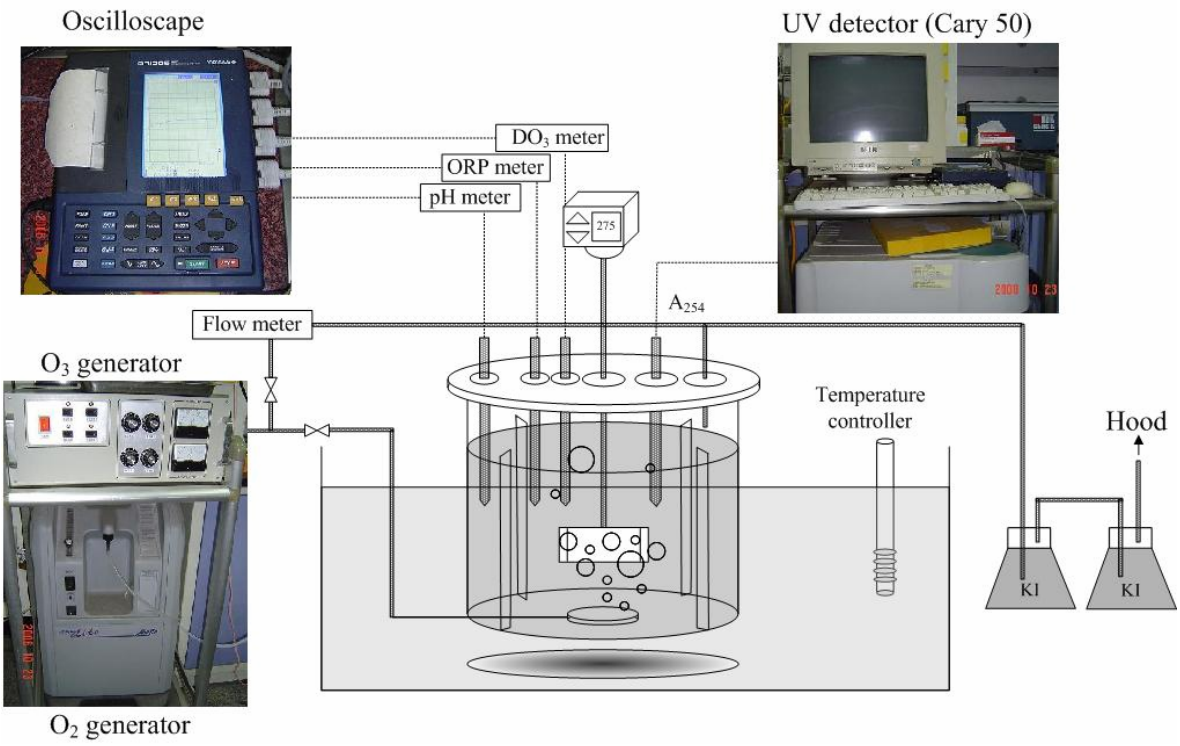

Figure 3.4 Schematic diagram of the 5-liter ozonation system equipped with a mixer and three monitor sensors (pH, ORP and dissolved ozone) connect with oscillographic recorder. Ultraviolet detector (Cary 50) connects with the optical fiber probe for monitoring the change of A_{254} in ozonation system.

3.2.4 On-line oscilloscope monitors equipment

The oscilloscope recorder with the pH and ORP sensors can be used to directly collect a number of instantaneous ORP and pH profiles in a personal computer by using the WaveStar^{TM} Software. The comprehensive data collection system can be 16,000 data points per second, which is very helpful to understand the rapid direct and indirect ozone reactions. The on-line spectrophotometer equipped with an UV detector and optical fiber probe also collected huge amount of A_{254} data during ozonation. The general information of ORP analysis conditions by using the Digital storage Oscilloscopes is summarized in.

Table 3.2 ORP analysis conditions by the Digital storage Oscilloscopes

Equipment	Specification and Operation Conditions
Digital storage Oscilloscope	Yokogawa, OR100E, Japan
Channel	Four channel
Frequency	60 MHz
Scan rate	1 Gs/S
Data collected	16,000 data storage per second

3.3 Analysis Methods

3.3.1 Basic water quality analysis

Basic water analysis is referring to NIEA (ROC) and Standard Methods, 21st Ed., (APHA *et al.*, 2005). The items for analysis of this study are pH, temperature, DO, TDS, COD, conductivity, hardness, alkalinity, NH_3-N and ORP. The items of the corresponding methods are listed in Table 3.3.

Table 3.3 Basic water quality analysis items and methods

Items	Methods and Instrument
pH	Electrode method (NIEA W424.50A)*; pH meter, (Suntex, TS-1)
Temperature	Thermometer method (NIEA W217.51A)
DO	DO meter (WTW, Microprocessor, Oximeter 4500G)
TDS	Conductivity meter (WTW, Conductivity meter, LF95)
COD	Closed Reflux, Titrimetric methods (Standard Methods 5220C, 21st)**
Conductivity	Conductivity meter method (WTW, LF95, NIEA W203.51B)
Hardness	EDTA Titration method (Standard Methods 2340C, 21st)**
Alkalinity	Titration method (Standard Methods 12320B, 21st)**
NH_3-N	Titrimetric methods (Standard Methods 4500-NH_3, 21st)**
ORP	ORP meter (Suntex, TS-1, Standard Methods 2580B, 21st)**

*NIEA method is referred to the Environmental Analysis Laboratory, EPA, Executive Yuan, R.O.C.

** Standard Methods 21st Ed., by APHA *et al.* (2005)

3.3.2 Absorbance at wavelength of 254 nm

The on-line UV spectrophotometer (Cary 50, Varian Pty Ltd) equipped with an UV detector and an optical fiber probe is used to collect absorbance at 254 nm (A_{254}) during ozonation. The optical fiber probe connected with an UV detector was inserted into reactor to monitoring the data. The UV spectrophotometer connected with a personal computer, which can be used to the UV spectrophotometer and the Cary Win UV software, is used to set the monitoring conditions.

3.3.3 Dissolved organic carbon (DOC)

The analysis procedure of dissolved organic carbon (DOC) is according to the Standard Methods 21st Ed., 5310D (APHA *et al.*, 2005). The concentrations of DOC were determined by a TOC analyzer (Model 1010, OI., USA). The wet-oxidation method is suitable to analyze the dissolved organic matter in the water sample. The organic matter which can passed through the 0.45 μm membrane during filtration is defined as the DOC. The water sample is acidified by adding H_3PO_4 then purged by N_2 gas to remove the inorganic carbon and volatile organic carbons. After the oxidant (sodium persulfate, $Na_2S_2O_8$) was added to the digester, the mixture temperature is raised to 100 ºC. Then, the CO_2, which was

formed form the organic carbons is passed through a dried oven for analytic form NDIR (nondispersive infrared spectrometery) to quantatine analytic of the DOC concentration. The reagents and equipment for DOC analysis are summarized in Table 3.4. The calibration data of DOC analysis is shown in Table 3.5.

Table 3.4 Summary of the reagent and equipment for DOC test

Reagent	Series Number, Maker, Country
$Na_2S_2O_8$	R. D. H., Germany
H_3PO_4	R. D. H., Germany
KHP	R. D. H., Germany
Equipment	Series Number, Maker, Country
TOC	Model 1010 O.I. Analytical, USA

*Stock solution: 2.128 g KHP in 1 L reagent water (1,000 mg-C /L)

Table 3.5 Summary of the calibration equation for DOC (2006.10.14)

Conc. (mg/L)	Volume (mL)	Peak Area	MDL** (mg/L)
0	20	1,055*	
0.5	20	12,013*	
1.0	20	20,970*	0.01
2.0	20	38,613*	
5.0	20	94,791*	
Calibration Curve			R^2
y = 18576x + 1908.6			0.999

*n = 3

** MDL: Choice a concentration which is slightly higher than the lowest concentration in calibration curve and analysis repeat 7 times. The MDL value, the 3 times of standard deviation (the data of 7 replicate analyses), is conversed into concentration unit and divided by slope.

3.3.4 Hydroxyl radicals determination

Coumarin at the highest purity grade was obtained from Aldrich Chemicals (C4261, USA). The HPLC system with reverse phase column for the chromatographic analysis is consisted of an UV-975 type detector and a PU-980 type pump (Jasco Co., Japan). The chromatographic data acquisition system software is used to control the HPLC system. The column is a Pharmacia C2-C18 μRPC column ST 4.6/100 with and a column volume of 1.66 mL. For all HPLC analysis,

the elution solution consisted of methanol and deionizer water (V/V=70:30) was used with flow rate of 0.5 mL/min. In all cases, at least 1,000 μL of solution was introduced into a 300 μL injection loop, to ensure a better quantification of the products. Before injection, the water sample was filtered through 0.45 μm membrane. The absorbance is measured at wavelength 275 nm, which is chosen in order to obtain the maximum sensitive detection towards coumarin. The calibration data of coumarin analysis is shown in Table 3.6.

Table 3.6 Summary of the calibration equations for coumarin (2007.03.05)

Coumarin* (mg/L)	Peak Area
0	10345
5	188426
20	766568
35	1367085
50	1929952
65	2470873
100	3.6×10^{-6}
Calibration equation: $y = 36409x + 46745$, $R^2 = 0.998$	
MDL**(mg/L) = 0.15	

*n = 3

** MDL: Choice a concentration which is slightly higher than the lowest concentration in calibration curve and analysis repeat 7 times. The MDL value, the 3 times of standard deviation (the data of 7 replicate analyses), is conversed into a concentration unit and divided by slope.

3.3.5 Preparation of magnetic superparamagnetic perfluorooctanoic acid-type catalyst

The magnetic perfluorooctanoic acid (MPFOA) are prepared in four sequential steps: (1) the formation of magnetite (Fe_3O_4) by means of the chemical precipitation; (2) coating iron oxide with silica to form the silica-coated magnetite by using the Stöber method (Stöber, 1968); (3)

formation of alumina particles by using sol-gel method; and (4) the perfluorooctanoic acid coated by heating to magnetic alumina particles. Figure 3.5 indicates the schematic diagram of experimental system for the synthetic processes. The solid core catalyst particles are prepared by using the chemical precipitation method from the magnetic $FeCl_3 \cdot 6H_2O$ and $FeCl_2 \cdot 4H_2O$ with the molar ratio of 2 : 1. Stoichiometrically, 1 mol magnetite is obtained by the addition of ammonia solution to alkalize the solution for formatting of precipitate in an inert atmosphere under rapid mixing (295 rpm). The chemical precipitation process was kept temperature at 80 ^{o}C for 3 minutes. Then, the magnetite formed particles were separated from the solution by a magnet and washed several times with distilled water. Subsequently, the obtained magnetite was contacted with a sodium silicate solution.

Stöber method was modified as following: the process for coating the magnetite particles with silica is carried out in a basic isopropoxide/water mixture under the room temperature. The Stöber method is used for coating iron oxide with silica to form the silica-coated magnetite. The magnetic particles were washed with water, then sink in isopropylalcohol and aqueous ammonia. Then it was dispersed

homogeneously by an ultrasonic vibration in water bath. Finally, under continuously mechanical stirring, teraethylorthosilicate (TEOS) was slowing dosed will well dispersing. After stirring for five hours, silica was formed on the surface of magnetite particles through condensing TEOS hydrolyzing and following by processes. The magnetic iron oxide/silica (Fe_3O_4/SiO_2) particles then were obtained.

In the sol-gel method, SiO_2/Fe_3O_4 particles, aluminum isopropoxide in isopropanol were mixed in the reactor under ultrasonic shaking for 20 minutes. Then, isopropanol-water mixture was dosed into the reactor at the rate of 3 ml/min. Then the magnetic iron oxide/silica/alumina particles can be obtained. The reaction between magnetic iron oxide/silica/aluminum particles and perfluorooctanoic acid aqueous solution was carried out at 60 ^{o}C for 4 hours. The obtained magnetic iron oxide/silica/alumina/perfuorooctanoic acid particles were defined as MPFOA particles.

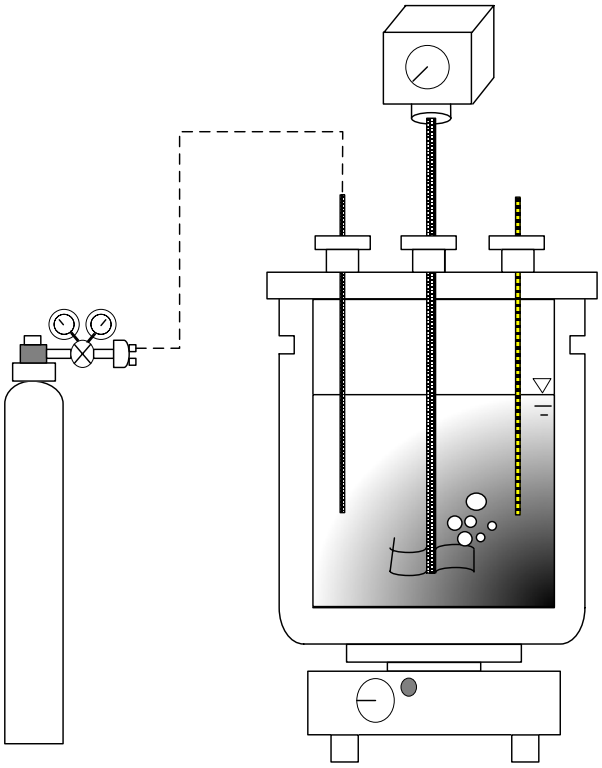

Figure 3.5 Schematic diagram of experimental system for the preparation experiments. The system contains: nitrogen purge injector, mixer, the thermometer and heating plate.

3.3.6 Scanning electron microscopy with energy dispersive spectrometer (SEM/EDS)

The field-emission scanning electron microscope (JSM-6700F, JEOL, Japan) is equipped with the cold field emission electron gun. The cold field emission electron gun is better than other thermal and Schottky electron guns because of low energy of dispersion of electron beam resulting in letter solution under a vacuum condition. The scope is also

equipped with the energy dispersive spectrometer (EDS); the results can be used for quantitative and qualitative analysis for materials.

3.3.7 Superconducting quantum interference device (SQUID)

Magnetic characterizations of particles were performed by means of a superconducting quantum interference device (SQUID) magnetometer (Model: MPMS5, Quantum Design Company, USA). The magnetization curves obtained from the SQUID magnetometer. The experiments were carried out at 25 ^{o}C, with additional magnetic field of 0 ~ 10 Gauss. The instrument specifications: temperature range of 2 ~ 400 K and magnetization range of 5×10^{-8} ~ 300 emu.

3.3.8 X-ray powder diffractometer (XRD)

A crystallographic study on MPFOA powder is performed by a rotating anode X-ray diffractometer (PHILIPS, X'pert MRDPRO) using a Cu Kα radiation. The distances between peaks, *d*, are calculated according to Bragg's law and are compared to the X-ray diffractometer data in order to deduce the crystal structure.

3.3.9 Fourier Transform Infrared Spectrometer (FTIR)

The IR spectra of MPFOA were obtained by using of a FTIR 460 plus analyzer (Jasco Co.) to obtain the FTIR spectra. The guided mixture of freeze-dried sample powder and bromide (KBr) at weight ratios about 1: 100-200, was pressurized to form a transparent thin slice. The transmittance spectrum is scanned over the wave number from 400 to 4,000 cm^{-1} and then processed by using KnowItAIR Information System 3.0 (Bio-Rad Laboratories, Inc.) software to transfer the interfecogram into the spectrum.

3.3.10 Carbon-13 Nuclear Magnetic Resonance (CPMAS ^{13}C NMR) spectrometer

CPMAS ^{13}C NMR experiments are carried out by using a Bruker AVANCE 400 spectrometer operated at a frequency of 100.63 MHz under a constant temperature of 300 K throughout all experiments. The NMR operating conditions are shown as follow:

1. Operating frequency: 100.63 MHz.
2. Recycle delay time: 1 sec.

3. 90° pulse width for ^{1}H excitation is 4 μsec, which corresponds to a $B_{1,H}$ field strength of 60 KHz.
4. Contact time: 1 msec.
5. Acquisition time: 0.037 sec.
6. Spectral width: 414.696 ppm.
7. Number of scans 80,000
8. Magic angle spinning frequency was consistently used as reference frequency.

Chapter 4 Results and Discussion

4.1 Water quality of Te-Chi Reservoir

Te-Chi Reservoir is the primary water source for Taichung area. In order to create the high profit agriculture output, a number of farmers extensively develop the fruit in the area of the upstream of water source. Those exploitations of steep mountainside caused the erosion of mudslide and driftwoods flow into the reservoir. Furthermore the excess pesticide and fertilizer applied on the field around the reservoir are also flowing into it along with top soil, which caused the degradation of reservoir water quality.

Table 4.1 shows the analytic data of Te-Chi Reservoir during the years between 1998 and 2006. The pH value is between 6.8 and 8.9, which is slightly higher than the average pH (6.0-8.5) from the reservoirs in Taiwan. During the past few years, the pH value is rising it might be resulted from the carbon dioxide consumption by algae the abundant amount of in the daytime. The range of the temperature is between 15.8 to 24.1 ^{o}C. The DO value is 10.5 mg/L, which higher than the previous level (5.2-8.7 mg/L) due to the algae blooming. While TDS value is 18 mg/L, which is far below the average TDS value of 500 mg/L.

The values of COD, hardness and the alkalinity are 6 mg/L, 125 mg $CaCO_3$/L and 120 mg $CaCO_3$/L, respectively. White, the standard (on average) values for COD, hardness values are 25 mg/L, and 300 mg as $CaCO_3$/L, respectively, for Taiwan water source. All of the analytic data are below the standard values.

Table 4.1 The water quality parameters of Te-Chi Reservoir raw water in recent years (1998-2006)

Item	pH	Temp	DO	TDS	COD	DOC	Conductivity	Hardness	Alkalinity	NH_3-N
Unit		℃	mg/L	mg/L	mg/L	mg/L	μs/cm	mg as $CaCO_3$/L	mg as $CaCO_3$/L	mg NH_3-N/L
Taiwan EPA std.*	6.0-8.5	-	≧6.5	≦500	≦25	≦4	-	≦300	-	≦0.1
1998	7.8	15.8	7.8	-	4	2	228	-	-	-
1999	8.7	24.1	8.7	177	-	2	196	113	150	0.1
2000	6.8	16.8	8.2	118	-	2	241	122	250	-
2001	8.0	23.0	8.3	106	12	1	240	94	81	0.4
2002	7.6	20.4	6.5	139	15	2	282	163	113	0.1
2003	8.5	22.6	5.8	164	13	1	333	160	25	0.1
2004	8.3	23.4	5.2	138	15	5	276	153	30	0.1
2005	8.0	22.6	8.0	26	4	5	51	131	2	0.1
This study, 2006	8.9	23.0	10.5	18	6	4	42	125	2	0.1

* The drinking water quality standard of Taiwan EPA (2005)

In order to understand the distribution characteristics of the nature organic matters (NOMs) in Te-Chi Reservoir water, the method proposed by Thurman and Malcolm (1981) was adapted to extract the water sample by using of XAD-8 resins. The extracted organic matters are divided into five categories, HAs, FAs, hydrophobic bases, hydrophobic neutrals and hydrophilic fractions. The percentages of these five organic matters obtained from the Te-Chi Reservoir raw water are shown as Figure 4.1. The fractions of hydrophobic and hydrophilic portions were 89.8 % and 10.2 %, respectively. The chemical structures of hydrophilic fractions are relative simple and can be degraded easily by microorganism. Kim and Yu (2005) reported that the hydrophobic fraction could be easily removed than the hydrophilic fraction by the conventional water treatment process.

Hydrophobic fractions include HAs, FAs, hydrophobic neutrals and hydrophobic bases. In this study, the percentage of HAs, FAs, hydrophobic neutrals and hydrophobic bases are 29.5 %, 19.5 %, 37.9 % and 2.9 %, respectively. In water body, the source of hydrophilic fractions contains the products from algae metabolism and artificial pollution. The more hydrophilic fraction means the more artificial waste

water pollution contains.

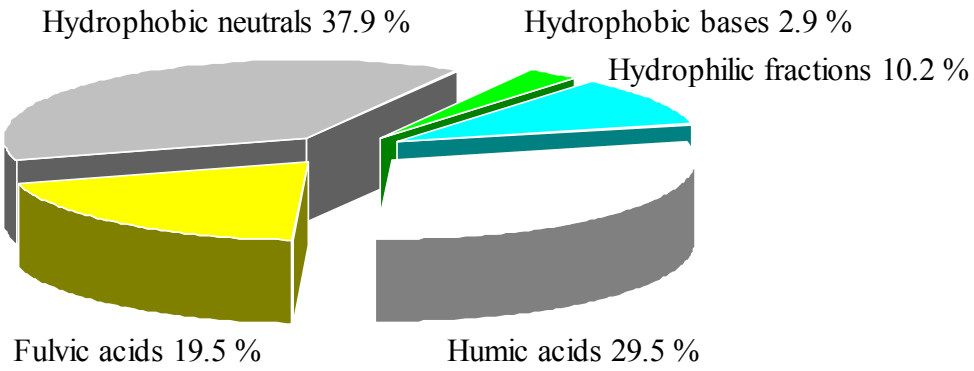

Figure 4.1 The percentage of five species (HAs, FAs, hydrophobic bases, hydrophobic neutrals and hydrophilic fractions) of organic fractions extracted from Te-Chi Reservoir in 2006.

The distributions of NOMs from Te-Chi Reservoir in recent years along with other literatures are shown in Table 4.2. On August 7-10, 2006, Bopha and Saomai typhoons brought heavy mudslide and floating woods into Te-Chi Reservoir. Therefore, the water body contained a lot of hydrophobic matters which are the products from the degradation of by floating matters. Comparing with the recent references (Table 4.2), the percentage of HAs and FAs increased obviously from 7.5 % to 29.5 %

and 11.3 % to 19.5 %, respectively. During the sampling time, many floating materials presented on the water surface, therefore, the HAs and FAs may be higher than the previous findings. This also causes the higher hydrophobic (89.8 %) than hydrophilic (10.2 %) fraction in this study. Huang *et al.* (2005) found that the distributions of hydrophobic and hydrophilic fractions in NOMs are 41.6 % and 58.4 %, respectively, from Feng-San Reservoir, Taiwan. Kim and Yu (2007) proposed the percentage hydrophobic and hydrophilic fractions are 47.2 % and 52.8 % respectively in Han River, Korea. The high hydrophilic portion means the water body contaminated by the artificial pollution. The high of hydrophobic fraction (89.8 %) implies the potential pollution came from the natural erosion mainly in upstream of Te-Chi Reservoir.

Table 4.2 The percentage distribution of Te-Chi Reservoir NOMs (% of DOC) in recent years (2001-2006) and compare to literature

Reference, Fraction (%)	HAs	FAs	Hydrophobic neutrals	Hydrophobic bases	Hydrophilic fractions
2001	7.5	11.3	24.1	1.4	55.5
2002	8.0	11.0	26.0	1.0	53.0
2003	10.0	11.6	26.0	1.6	49.5
2004	24.3	7.9	25.2	2.2	40.4
2005	29.7	19.5	31.2	2.6	15.7
This study, 2006	29.5	19.5	37.9	2.9	10.2
	Hydrophobic fractions				Hydrophilic fractions
Huang, *et al.*, (2005), Feng-San Reservoir, Taiwan	41.6				58.4
Kim and Yu (2007), Han River, Korea	47.2				52.8
Bose and Reckhow (2007), Forge Pond, Granby, MA, USA	54.2				33.1
This study, 2006	89.8				10.2

The SUVA (specific ultraviolet absorbance, the ratio UV absorbance divided by DOC) is often used to indicate the level of aromatic materials in humic acid. Chow (2006) reported that SUVA correlates with the level of aromatic carbon and phenolic contents and has been widely used as a surrogate parameter in determining the aromatic substance of natural organic matter.

Figure 4.2 shows the profiles of SUVA for raw water and five extracted organic fractions (HAs, FAs, hydrophobic neutrals, hydrophobic bases and hydrophilic fractions) from Te-Chi Reservoir. The specific absorbance value of hydrophobic fractions is higher than that of hydrophilic fractions. Among hydrophobic fractions, HAs (0.018 abs/mg) and FAs (0.006 abs/mg) display the higher value than other species. Bose and Reckhow (2007) observed that the content of unsaturated bond in HAs and FAs is higher than other fractions. Therefore, the higher A_{254} in organic matter implies the more unsaturated bond structure, i.e., C=C or aromatic, exists. On the contrary, SUVA value of hydrophilic fractions is less than 0.004 abs/mg, indicates the content of unsaturated bond. Kitis *et al.* (2002) also found that the SUVA value of hydrophobic fraction (0.046 abs/mg) is higher than that

of hydrophilic fraction (0.020 abs/mg) in water treatment plant in Myrtle Beach, South Carolina, USA. The hydrophobic fractions exhibited higher SUVA than that of the hydrophilic fractions. This means that hydrophobic species consisted of more aromatic (unsaturated) structured components than that of hydrophilic fractions and therefore have higher potential to form disinfection by-products.

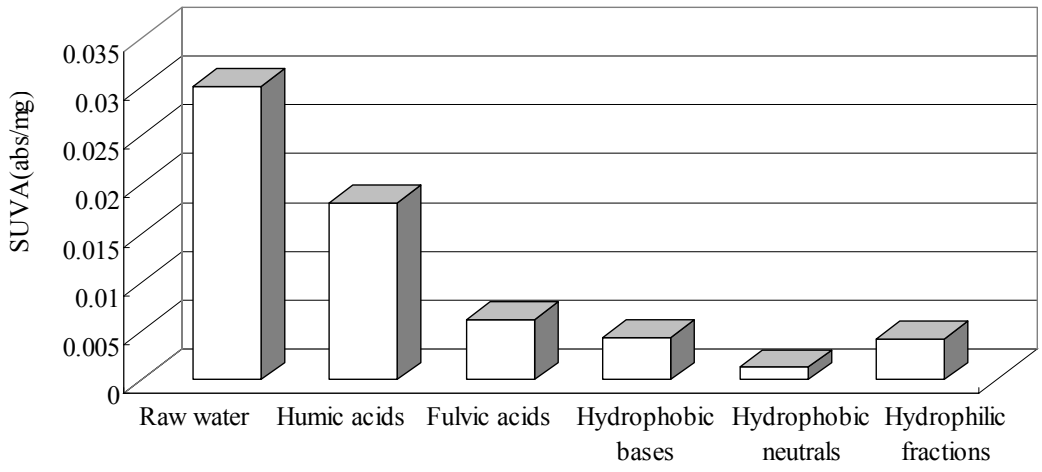

Figure 4.2 The SUVA value (A_{254}/DOC) of raw water and five fractions (HAs, FAs, hydrophobic bases, hydrophobic neutrals and hydrophilic fractions) extracted from Te-Chi Reservoir in 2006.

4.2 Characteristics of preparation magnetic perfluorooctylalumina (MPFOA) catalyst

4.2.1 Specific surface area

The specific surface area of the synthetic magnetic catalyst particles are determined by the measurement of N_2 gas adsorption at 300 K with an automatic adsorption instrument (SA3100, Florida, USA) and calculated by the Brunaure-Emmett-Teller (BET) equation. The BET surface area of the preparation magnetic catalyst (MPFOA) particles is 80 m^2/g with the diameter of 10 μm and the pH_{zpc} of 5.5.

4.2.2 Magnetic particle patterns

The SEM images and EDS spectra of the pre catalyst and catalyst particles are shown in Figure 4.3. The particle surfaces are shown close to a uniformly spherical. Figure 4.3 (a) shows the SEM picture and EDS spectrum of t Fe_3O_4/SiO_2 particles with the diameter about 100 and 200 nm. The atomic percentage of Si is 19.0 % and Fe is 7.3 % from the Table 4.3. While according to Figure 4.3 (b), particle surfaces of $Fe_3O_4/SiO_2/Al(OH)_3$ are larger than that obtained from its precision. In this stage, the $Fe_3O_4/SiO_2/Al(OH)_3$ particle diameters are between 300

and 400 nm, and the atomic percentage of Al is 21.6 %, Si is 3.2 % and Fe is 0.7 %. The Figure 4.3 (c) shows the final synthetic product of MPFOA. Although, the MPFOA particle surfaces are not uniform, the apparent diameters are larger than previous products which shown in Figure 4.3 (a) and (b). The atomic percentage MPFOA of Fe is 8.6 %, Al is 6.7 %, Si is 5.7 % and Fe is 1.6 %. Therefore, the synthesized magnetic catalyst particles (Figure 4.3 c) in this study are covered with the atomic contents of Fe, Si, Al and F, respectively.

(a) Fe_3O_4/SiO_2

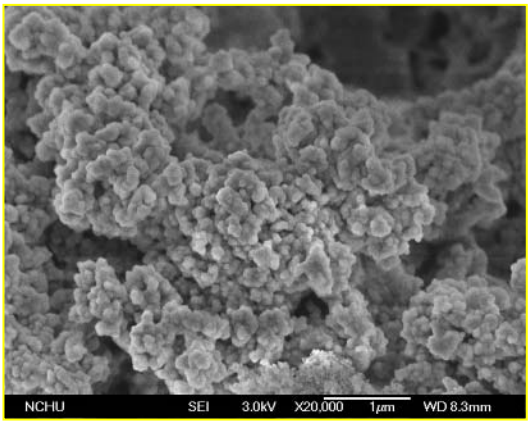

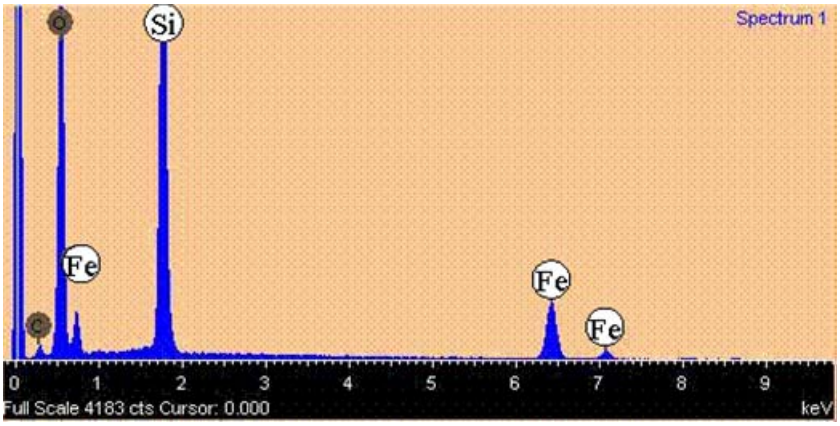

(b) $Fe_3O_4/SiO_2/Al(OH)_3$

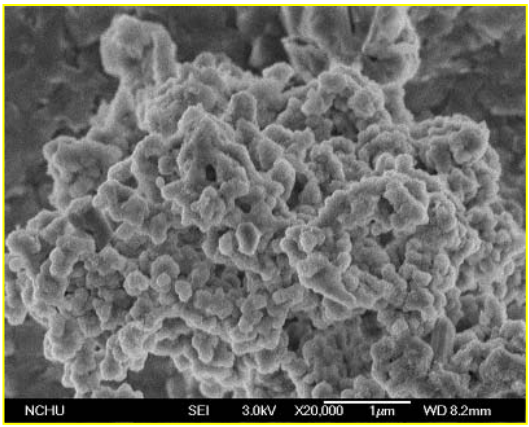

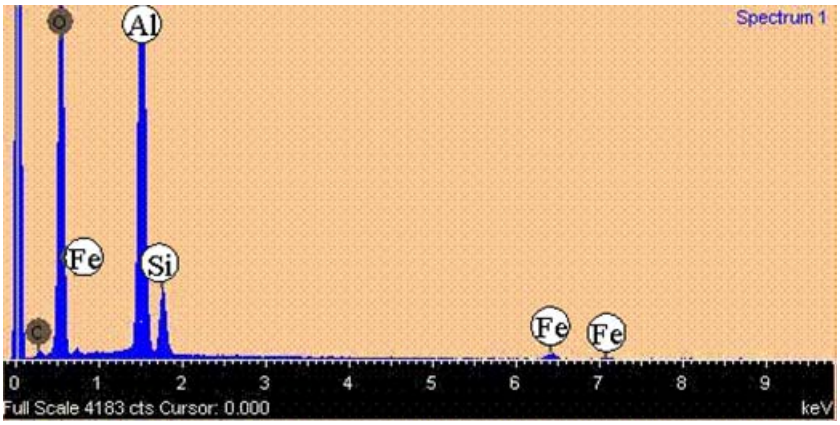

(c) MPFOA

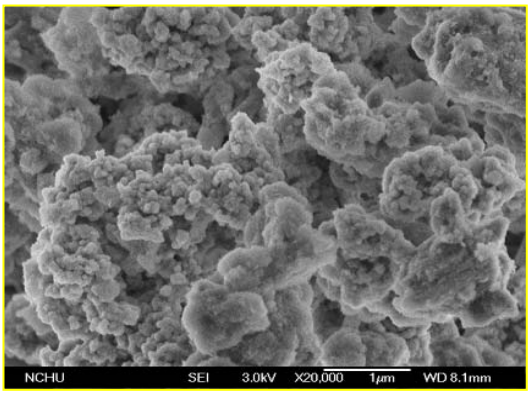

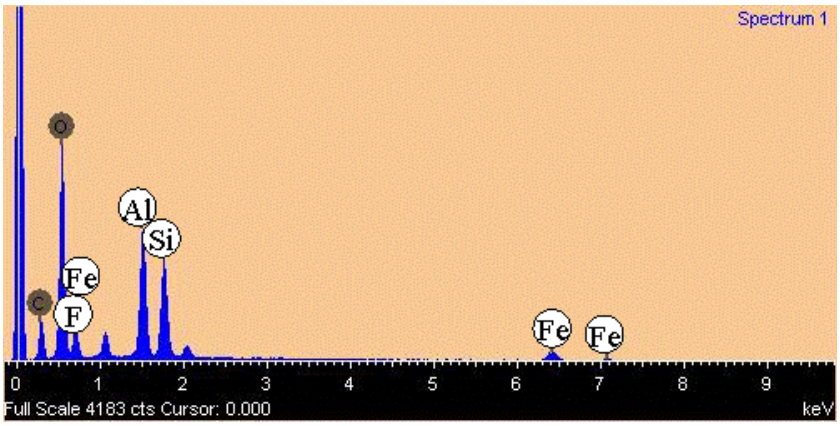

Figure 4.3 The SEM pictures and EDS spectra of (a) Fe_3O_4/SiO_2, (b) $Fe_3O_4/SiO_2/Al(OH)_3$ and (c) MPFOA.

Table 4.3 The EDS spectra of atomic percent of the intermediates (a, b, c) along the preparation of MPFOA

Element	Atomic, %		
	(a) Fe_3O_4/SiO_2	(b) $Fe_3O_4/SiO_2/Al(OH)_3$	(c) MPFOA
Fe	7.3	0.7	1.6
Si	19.0	3.2	5.7
Al	-	21.6	6.7
F	-	-	8.6

4.2.3 Magnetization curves

The magnetization curves obtained from the SQUID magnetometer are shown in Figure 4.4. The results reveal that the intensities of the saturation magnetization (*Ms*) of Fe_3O_4, Fe_3O_4/SiO_2, $Fe_3O_4/SiO_2/Al(OH)_3$ and MPFOA particles are 76.6, 26.8, 15.7 and 0.008 emu/g, respectively. Furthermore, all the magnetic particles possess superparamagnetism because of the zero coercive force and being free of hysteresis.

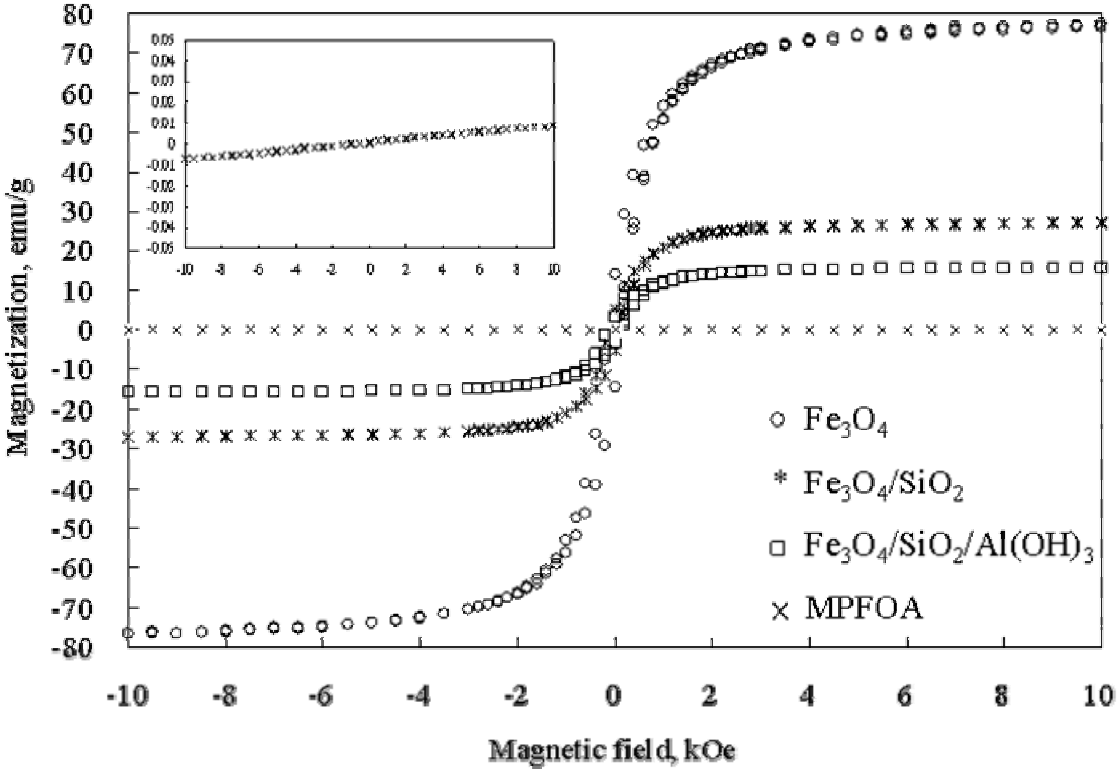

Figure 4.4 Magnetization curves of various magnetic particles.

4.2.4 Crystal structure of magnetic particles

The XRD patterns of various magnetic particles are illustrated in Figure 4.5 with. Sun *et al.* (2005), Deng *et al.* (2005) and Charvin *et al.* (2007) reputed that the Fe_3O_4 will display six peaks in the XRD patterns within 2θ scale as showing in Figure 4.5 (a). The similar peaks are observed along with additional peaks in the profile Figure 4.5 (b) and Figure 4.5 (c), this indicates the presence of crystal Fe_3O_4 in the intermediates. Almost identical peaks in both Figure 4.5 (a) and 4.5(c)

indicate that the crystal structure of Fe_3O_4 in the Fe_3O_4/SiO_2 particles is almost not changed during the coating process although the presences of small variation of intensities of the main and minor peaks were appeared. The peaks between 15 and 25^o of 2 θ seam range can be interpreted as the reflection of the amorphous form silica in Fe_3O_4/SiO_2 particles is amorphous (Lou *et al.*, 2006). In Figure 4.5 (c) above that the crystal aluminum is existence in the magnetic particles, i.e., Bayerite of $Fe_3O_4/SiO_2/Al(OH)_3$, which is also observed form Figure 4.5 (d). Therefore, the magnetic catalyst particles in this study the layers sequence from the center to outer layers are Fe_3O_4, amorphous SiO_2 and Bayerite, respectively.

(a) Fe_3O_4 (b) Fe_3O_4/SiO_2

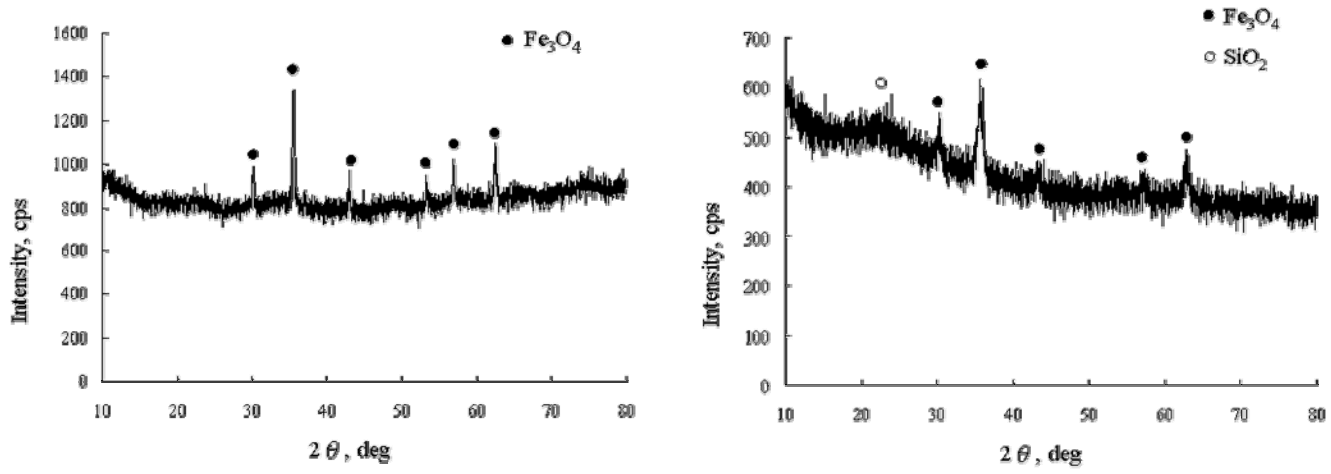

(c) $Fe_3O_4/SiO_2/Al(OH)_3$ (d) MPFOA

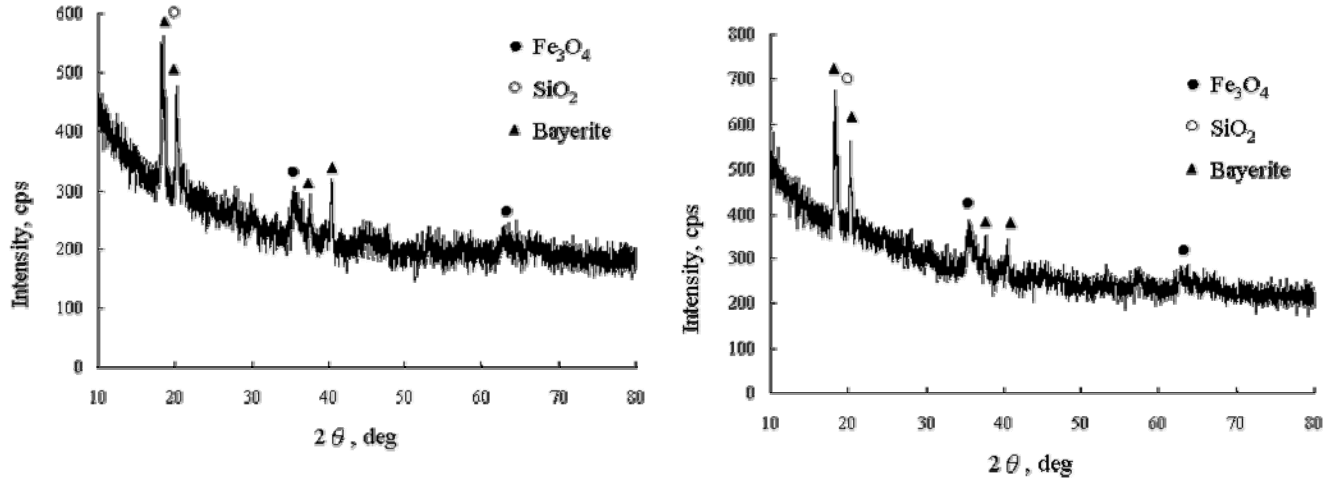

Figure 4.5 X-ray diffraction (XRD) patterns with the radiation source of Cu Kα for various magnetic particles: (a) Fe_3O_4 particles; (b) Fe_3O_4/SiO_2 particles; (c) $Fe_3O_4/SiO_2/Al(OH)_3$ particles and the final product of (d) MPFOA particles.

4.2.5 The characteristics and recycling test of the catalyst MPFOA

The FTIR spectrum of pure perfluorooctanoic acid (PFA) and assembled MPFOA are shown in Figure 4.6. The typical absorption for C-F bonds stretching is located between 1,100 to 1,250 cm^{-1} for both

perfluorooctanoic acid and MPFOA according to Wieserman *et al.* (1991). This implies that the MPFOA (Figure 4.6 (b)) are acceptable based on the FTIR analysis. In addition to the C-F stretching symmetric Si-O-Si bond stretch (800 cm^{-1}) in the spectra of silica and iron oxide-silica nanocomposites (680 and 900 cm^{-1}) is consisting to the citation by Ehrman *et al.* (1999). The FTIR spectrum of the recycle MPFOA is also shown in Figure 4.6 (c); which indicates that the characteristics of the recycled MPFOA are compatible to the fresh MPFOA (Figure 4.6 (b)). The characteristics absorption, i.e. 3400, 1700 and 1,100 to 1,250 cm^{-1}, of MPFOA are also observed for the conformation about the extend of deterioration from fresh MPFOA. Both the fresh and recycled MPFOA are observed to display the similar absorption frequencies in the spectra patterns. Therefore, the recycled MPFOA is utilized for all the following tests in this study. Figure 4.6 (d), the abruption frequencies dry functional groups of MPFOA after 5^{th} recycled are still shown similar that to from the fresh MPFOA (Figure 4.6 (b)). Therefore, it can be concluded that the synthetic catalyst with the recovery ratio between 85-95 % can maintain the function after recycling.

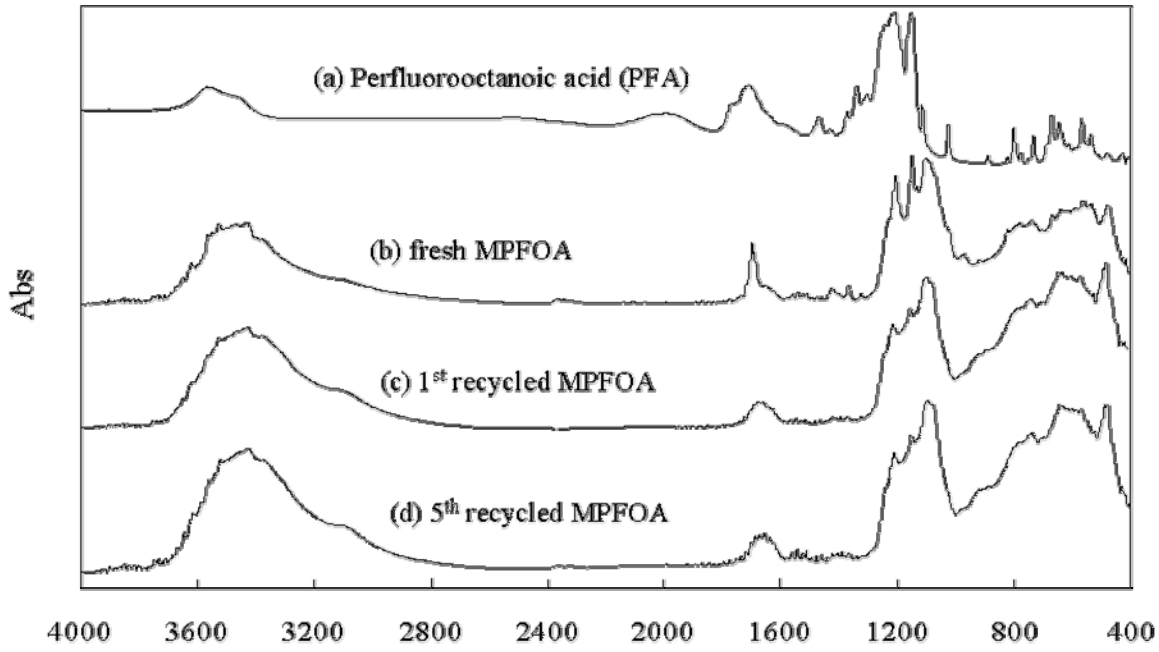

Figure 4.6 The FTIR spectra of (a) perfluorooctanoic acid (PFA), (b) fresh MPFOA, (c) 1st recycled MPFOA and (d) 5th recycled MPFOA. The main stretching frequencies for functional C-F bonds appeared between 1,100 to 1,250 cm^{-1}.

4.2.6 The dose of catalyst

Figure 4.7 shows the ORP profiles of 1 liter pure water during ozonation (blank), with 0.5, 1.0, 2.0, 3.0 and 4.0 g/L MPFOA as catalyst. The ORP value obtained from the reaction with the dose amount of 0.5 g/L is obviously slower than that from the dose of 1.0 g/L. The similar ORP profiles are found from the dose amount of 1.0, 2.0, 3.0 and 4.0 g/L MPFOA, i.e., all of the ORP values reached to 600 mV in 30 seconds contact time. However, without the presence of MPFOA (i.e. blank) the

ORP value will reach to 600 mV after 400 seconds contact time. Therefore, the 1.0 g/L of MPFOA is selected as the dosage for the following catalyst tests.

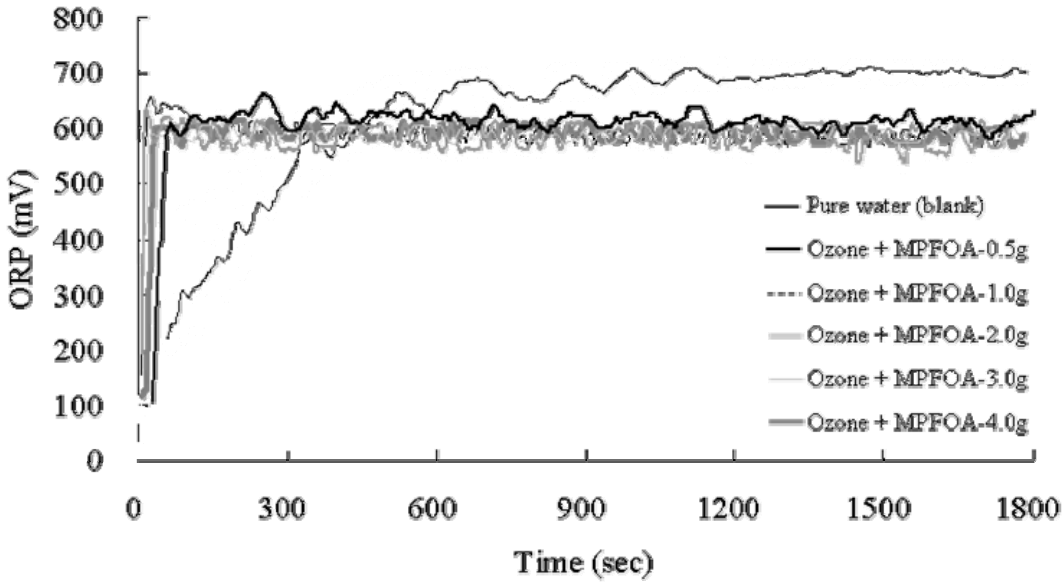

Figure 4.7 The ORP profiles of ozonation (blank) with the dose amount of 0, 0.5, 1.0, 2.0, 3.0 and 4.0 g/L of MPFOA.

4.3 The investigation of ozonation mechanisms

4.3.1 Hydroxyl radicals measurement

Among chemical oxidation processes, ozonation is a very high efficient method for the oxidation of toxic and refractory compounds. Kusic *et al.* (2006) and Meunier *et al.* (2006) showed that ozonation reaction consists of two steps, i.e. direct (ozone molecular) and indirect (free OH radicals) attacking processes. The measurement of free OH radicals is difficult, due to its short half-life which estimated to be around 10^{-9} s (Sarma *et al.,* 1996; Cheng *et al.,* 2002). Therefore, an unpaired electron, free radical, is highly unstable and immeasurable. Recently, many researchers proposed the free radicals analysis method with successful (Wojnárovits *et al.,* 2005; Newton and Milligan 2006).

Louit *et al.* (2005) indicated that the hydroxycoumarin isomers of 3-OH, 4-OH, 5-OH, 6-OH and 8-OH coumarins are also produced during the ozonation of the coumarin. HPLC can be used to detect the isomers of hydroxycoumarins and therefore, the free OH radicals can be measured indirectly. In this study ozone is continuously purged into pure water until the saturated level followed by adding of various coumarin concentrations (0-80 mg/L). The consumption of the amount of

coumarin is equivalent to the equivalent mole number of OH radical in water, i.e., each unit OH radicals combined with one unit coumarin. Figure 4.8 shows that the initial coumarin concentration (65 mg/L) been consumed equals to the maximum (1.6 mg/L) OH radical exists in the reactor.

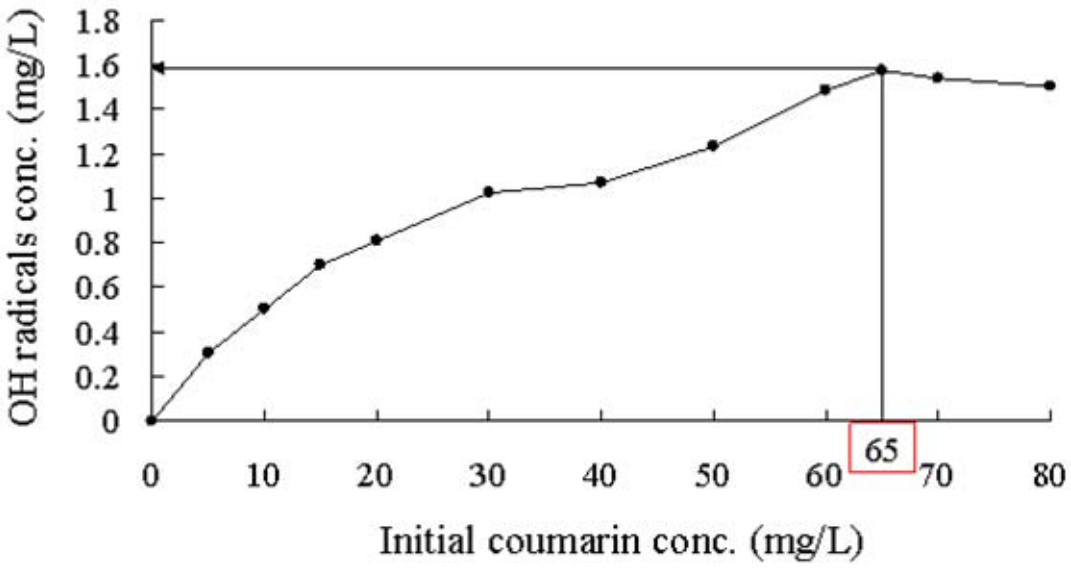

Figure 4.8 The maximum OH radicals (mg/L) in pure water during saturated ozone. The initial coumarin concentration (65 mg/L) indicates the maximum amount of OH radical (1.6 mg/L) in the reactor.

4.3.2 Ozonation and catalytic ozonation mechanisms

The on-line dissolved ozone, ORP, and pH are monitored by the oscilloscope continuously during the ozonation reaction. Figure 4.9 (a) shows the on-line monitored data of ORP and DO_3 during the ozonation and catalytic ozonation in a pure water system. Without presence of catalyst, the ORP value is increasing since introduction of ozone molecule. The ORP value rise from 200 mV to 650 mV during the period of 600 sec and keep in static level of 680 mV throughout the reaction. On the other hand, the catalytic ozonation, at the moment of injecting point, the ORP jumps to 650 mV and keep at static level throughout the reaction. Consequently, it can be concluded that the catalyst is able to enhance ozone (catalytic ozonation) reaction. During the reaction, the pure ozone and catalytic system are aerated continuously to a saturation level, while, at 300 sec, the concentrations of saturated ozone are 2.2 mg/L and 2.0 mg/L, respectively, with the water temperature of 25±2 ^{o}C. The amount of OH radicals presence in the solution is measured by using moles of the consumption coumarin in reaction. Therefore, Figure 4.9 (b) implies the OH radicals which reacted quantitatively with counarin. The maximum concentration of

OH radicals is around 1.6 mg/L and 1.4 mg/L, respectively during pure ozonation and catalytic ozonation.

(a) ORP and DO_3 of pure water

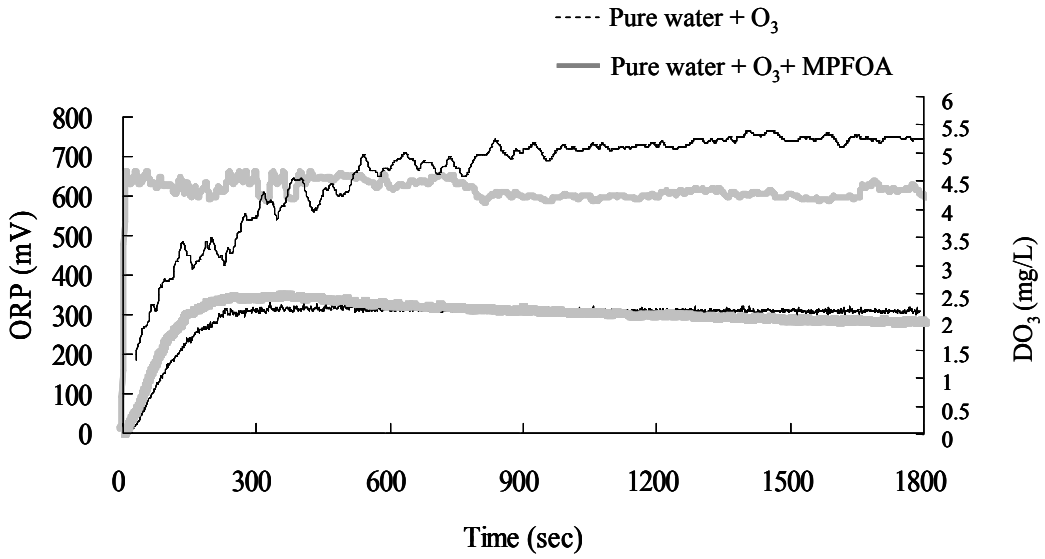

(b) OH radicals of pure water

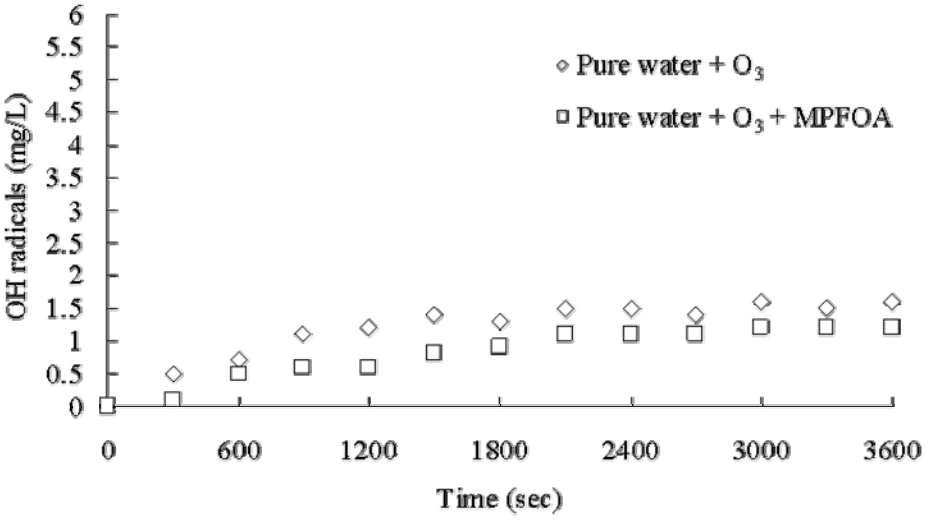

Figure 4.9 The analytic value on-line monitored data (a) ORP and DO_3, (b) OH radicals during the ozonation and catalytic ozonation of pure water.

Figure 4.10 shows the on-line monitored data of (a) ORP and OH radicals and (b) pH and DO_3 during the ozonation and catalytic ozonation of Te-Chi Reservoir raw water. Figure 4.10 (a) shows the catalytic ozonation system, in which the ORP value jumps to the maximum level of 640 mV with respect to 540 mV in the pure ozonation system while. In addition, the maximum concentration of OH radicals was around 1.6 mg/L on pure ozonation system. In ozonation with catalyst system the OH radicals was around 1.5 mg/L. Therefore, it can conclude that the MPFOA can enhance the stability of ozone during the reaction. Jen *et al.* (1998) reported that salicylic acid can be used as a scavenger followed lay analyzing by using HPLC to obtain the concentration of OH radicals at level around 1.9 mg/L. Figure 4.10 (b) shows that after the pure ozone aerated continuously to the saturation level, i.e., for 250 seconds, the dissolved ozone also reached to the saturated peak of 2.2 mg/L, while the ozone concentration was 2.0 mg/L for the catalytic ozonation system . The pH value does not change significantly and falls in the range between 7.5 and 7.8.

(a) ORP and OH radicals of Te-Chi Reservoir raw water

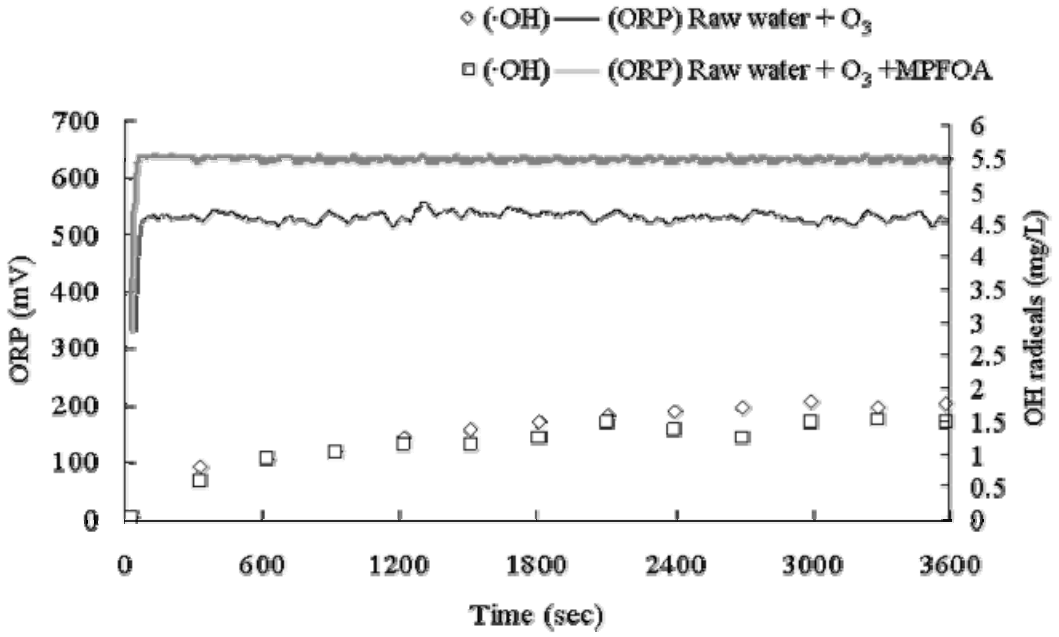

(b) pH and DO_3 of Te-Chi Reservoir raw water

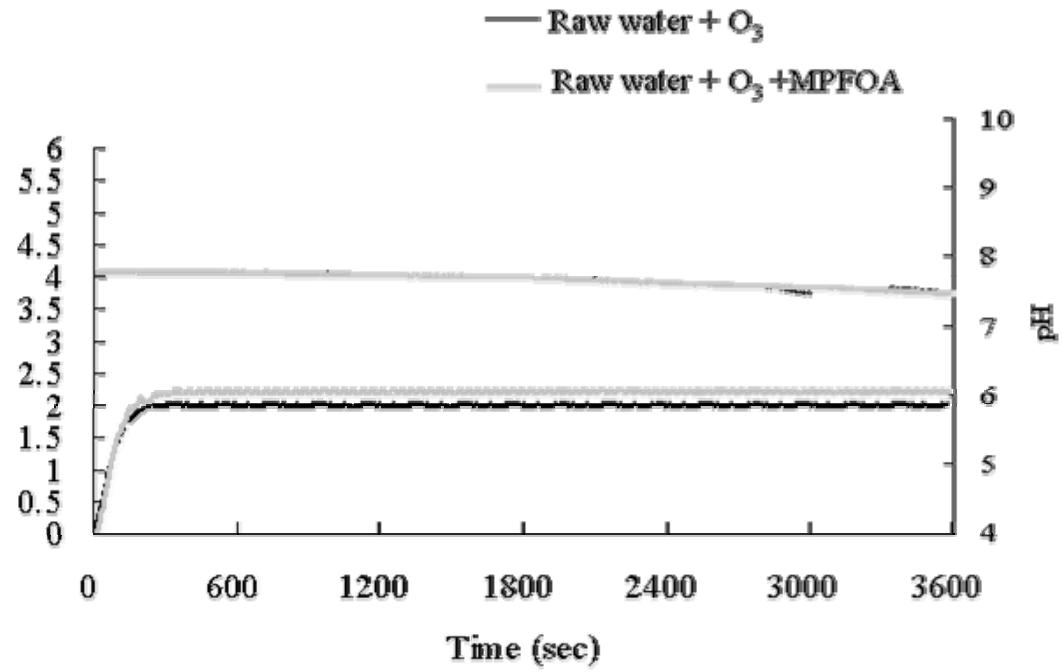

Figure 4.10 The on-line monitored data (a) ORP and OH radicals, (b) pH and DO_3 during the ozonation and catalytic ozonation of Te-Chi Reservoir raw water.

4.4 Modeling of ozonation and catalyst system

The Nernst equation has been used to understand the redox reaction of molecule in solution (Hancock *et al.*, 2004). Nicoli *et al.* (2004) suggested that the ORP value represents the information about the real oxidation/reduction ability of a molecule and its prevalent form (oxidized or reduced) in the system. The derivatives of this model is attached in the Appendix I. of this Thesis.

Theoretically, the concentration of both the reactants and products can be represented by the measurement of A_{254}. The decrease of A_{254} during the ozonation implies the unsaturated double bond is consumed to from other saturated bonds. Therefore, the organic compounds ($C_xH_yO_z$) can be replaced by A_{254}. The amount of DO_3 and free OH radicals can be measured for the redox reaction equation. The Nernst equation can be expressed as Eq. 4.1.

$$E = a + b\ pH + c \ln\left[A_{254}\right]\left[O_3\right] + d \ln\left[\cdot OH\right] \quad \text{.....Eq. 4.1}$$

During the ozonation and catalytic ozonation, the model adapts the on-line A_{254} values determined at different time can be used for the treated Te-Chi Reservoir raw water. The Nernst equation is obtained as

following:

$$ORP = 450 - 4\,pH - 25\ln[A_{254}][O_3] + 5\ln[\cdot OH] \quad \text{.....Eq. 4.2}$$

$$ORP = 643 - 3\,pH - 4\ln[A_{254}][O_3] + 2\ln[\cdot OH] \quad \text{.....Eq. 4.3}$$

The model regression shows a satisfactory R-square value of 0.93 at pure ozonation. While the catalytic ozonation case yields an R-square value of 0.90. In this study, the Nernst model can be used to simulate the ozonation reaction. Due to the complicated organic matters, various types of target compounds need to be investigated in the future. Therefore, we suggests set up different types of modified Nernst equation for different cases, which can provide useful modeling information in the water treatment process.

The comparison of the predicted model and the on-line monitored ORP value is shown in Figure 4.11. Chang *et al*. (2004) have demonstrated that the ORP curve can be simulated by the modified Nernst equation under redox system. In this study, the R^2 of both these two modified model are above 0.995, which indicates the measured ORP curve can properly be approached by the form of modified Nernst Equation.

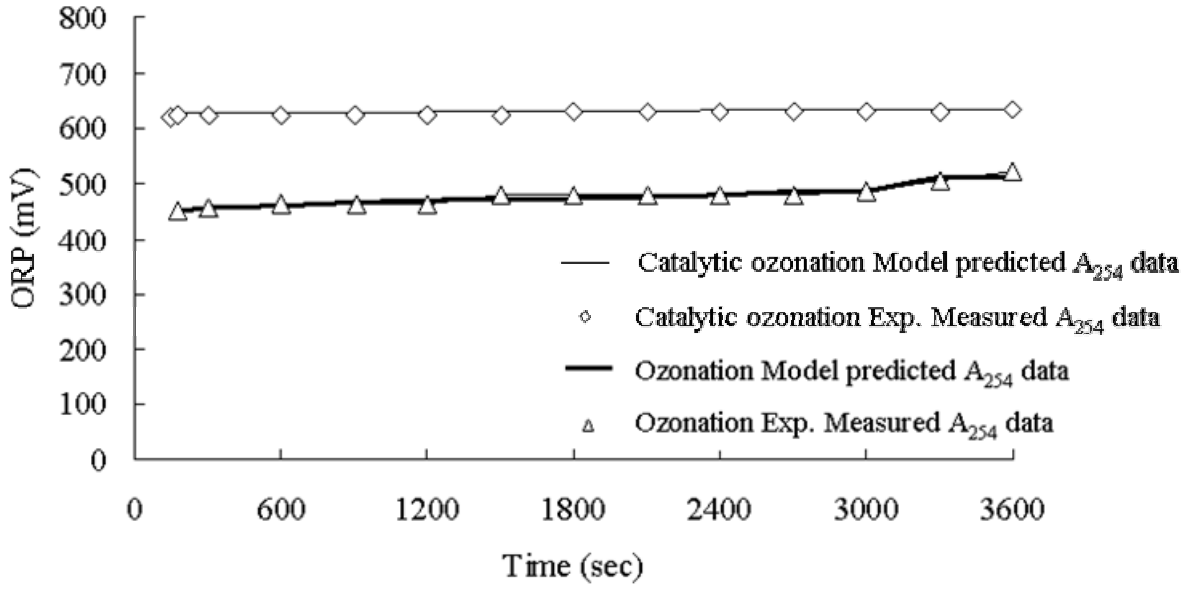

Figure 4.11 The Nernst model simulation of A_{254} during ozonation and catalytic ozonation of Te-Chi Reservoir raw water.

4.5 Change of functional groups during ozonation

Fourier transform infrared spectra (FTIR) and CPMAS Carbon-13 nuclear magnetic resonance spectra (^{13}C NMR) have been preciously applied for both qualitative and quantitative characterization of NOMs (Wiles *et al.*, 2007). In the interpretation of the functional groups, the FTIR is a crucial technical. The FTIR analysis of the isolated samples inform about the variation of functional groups within the organic fractions, which provides a basis for comparison of compositional differences between fractions. Table 4.4 is the abbreviated tables of the group frequencies for NOMs organic groups obtained by Lin *et al.* (2001), Hafidi *et al.* (2005) and Kanokkantapong *et al.* (2006). The table displays the information of the wave number function on the chemical bonds of the chemical compound. These identities ranges may be used to illustrate the FTIR spectra for investigating the variation of functional groups during the course of catalytic ozonation.

Table 4.4 Abbreviated tables of group frequencies for NOMs organic groups obtained by Lin *et al.* (2001), Hafidi *et al.* (2005) and Kanokkantapong *et al.* (2006)

Type of compound	Bond	Wave number (cm^{-1})
Alkanes	C-H (stretching)	2,850-2,970
		1,340-14,70
	-CH (Bending)	1,350-1,480
Alkenes	C-H (Stretch)	3,010-3,095
	=CH (Bending)	675-1,000
	C=C (Stretch)	1,610-1,680
Alkynes	C-H (Stretch)	3,300
	C≡C (Stretch)	2,100-2,260
Alcohols	O-H (stretch, H-bonded)	3,200-3,600
	O-H (stretch, free)	3,590-3,650
	C-O (stretch)	1,050-1,300
Alkyl Halide	C-F (Stretch)	1,000-1,400
	C-Cl (Stretch)	600-800
	C-Br (Stretch)	500-600
	C-I (Stretch)	500
Amines, amides	N-H (Stretch)	3,300-3,500
	C-N (Stretch)	1,180-1,360
Aromatic rings	C-H (Stretch)	3,010-3,100
		690-900
	C=C (Stretch)	1,500-1,600
Carboxylic acids	C-O (Stretch)	1,050-1,300
	O-H (Stretch)	3,500-3,600
	O-H (stretch, H-bonded)	2,500-2,700
	C=O (Stretch)	1,690-1,760
Ether	C-O (Stretch)	1,050-1,300
Ester	C-O (Stretch)	1,050-1,300
	C=O (Stretch)	1,690-1,760
Aldehydes, Ketones	C=O (Stretch)	1,650-1,750

Figure 4.12 shows the FTIR spectrums of Te-Chi Reservoir raw water (a) before ozonation (Raw water), (b) after ozonation (Raw water + O_3) and (c) after ozonation with MPFOA (Raw water + O_3 + MPFOA). The valleys on the transmittance curves are caused by the absorption of specific functional groups. In this study the main absorption peaks attributes to C-Cl and C-Br chemical bonds in alkyl halide (500-800 cm^{-1}), C-H chemical bonds in aromatic rings (810-900 cm^{-1}), C-O chemical bonds in alcohols, ester, ether and aromatic rings (1,050-1,300 cm^{-1}), -C-H chemical bonds in alkanes (1,350-1,480 cm^{-1}), C=C chemical bonds in alkenes (1,610-1,680 cm^{-1}), N-H chemical bonds in amines and amides (3,300-3,500 cm^{-1}) and O-H chemical bonds in carboxylic acids (3,500-3,600 cm^{-1}) (Hung, 2006; Chiang, 2005). The adsorption signal appears at 2,300-2,400 cm^{-1} corresponding to carbon dioxide peak from the air (Chien *et al.*, 2000; Qu *et al.*, 2007). Figure 4.12 is composed lay three FTIR spectra (a) Raw water service as the base for the comparison purpose, and (b) the organic component after ozonation reaction and (c) the organic components after ozonation with catalyst MPFOA. Increase of transmittance (%) means the strongly destroy of chemical bonds by enhancing the ozonation. The transmittance spectra

of the resultant from the ozonation (Figure 4.12 (b)) and ozonation with catalyst MPFOA reaction (Figure 4.12 (c)) display the similar trends, in which the chemical bonds have been destroyed for formation more debris of organic matters.

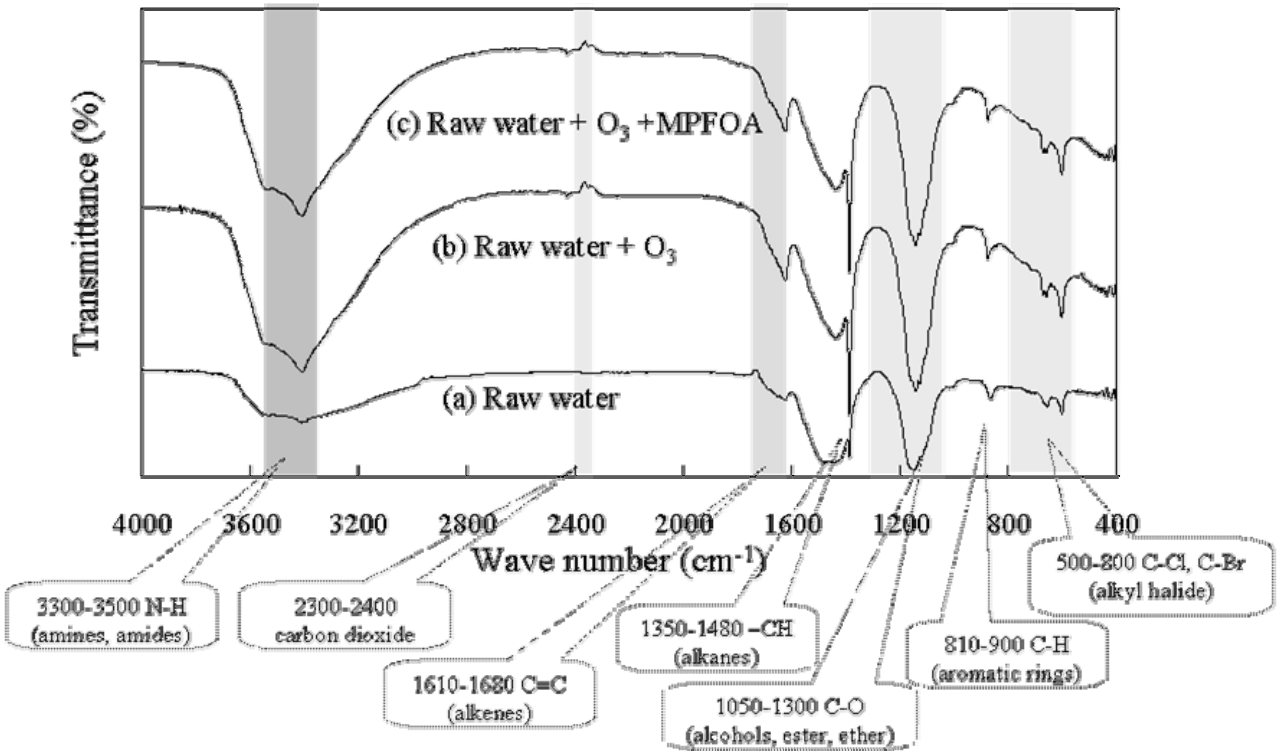

Figure 4.12 FTIR spectra of Te-Chi Reservoir raw water (a) before ozonation (Raw water), (b) after ozonation (Raw water + O_3) and (c) after ozonation with MPFOA (Raw water + O_3 + MPFOA).

Figure 4.13 shows ^{13}C NMR spectra of Te-Chi Reservoir raw water. The spectra contain the samples obtained (a) before ozonation (Raw water), (b) after ozonation (Raw water + O_3) and (c) after ozonation with MPFOA (Raw water + O_3 + MPFOA). DeLApp *et al.* (2005) and Hafidi *et al.* (2005) indicated the correlations between resonance signals in ^{13}C NMR spectra and the types of chemical groups as: alkyl region (0-50 ppm; methyl groups: around 20 ppm, saturated alkane chains: around 30 ppm, branched aliphatics: around 40 ppm); overlap region (50-60 ppm; methoxy groups: 56 ppm); O-Alkyl region (60-100 ppm; carbohydrate-derived: (71 ppm); aromatic; unsaturated region (100-160 ppm; substituted polyphenolic C: 105 ppm, unsubstituted aromatic C: 115 ppm, substituted aromatic C: 128 ppm, heterosubstituted: 150 ppm); carboxyl region (160-190 ppm; carboxyl groups: 171 ppm) and carbonyl region: (ketone: quinones: 195 ppm) (Hung, 2006; Chiang, 2005).

The spectra of Figure 4.13 can be separated into two main areas which corresponding to carbon associated with substituted polyphenolic carbons (95-105 ppm) and carboxyl/carbonyl carbons (155-175 ppm) (Hung, 2006; Chiang, 2005). The intense decreasing after ozonation shows the strong oxidation degraded ability of ozone molecule. Which

the addition of MPFOA for catalytic ozonation slightly higher decompose rater toward to carboxyl/carbonyl carbons than that obtained from the pure ozonation in raw water system. The resonance line between 95-105 ppm for C-substituted polyphenolic carbons was absence; it might result from the ultra low concentration of raw water. The other reason might be that the line between 155-175 ppm carboxyl/carbonyl carbons is too intense to make the other peaks indistinct. Whether the line belongs to inorganic or organic carbon need to further verify in the future.

This study also discusses the carbon associated matters from the decomposition of humic acid. Figure 4.14 ^{13}C NMR spectra of humic acid extracted from Te-Chi Reservoir raw water (a) before ozonation (Humic acids), (b) after ozonation (Humic acids + O_3) and (c) after ozonation with MPFOA (Humic acids + O_3 + MPFOA). In Figure 4.14 the two main peaks corresponding to carbon associated with saturated alkanes (20-30 ppm) and carboxyl/carbonyl carbons (163-190 ppm) (Hung, 2006; Chiang, 2005). The decrease intensity of resonance lines after ozonation shows the strong oxidation ability to consume more obis soled organic carbon. While the situation under addition of MPFOA catalyst addition case, the peak of saturated alkanes and

carboxyl/carbonyl carbons also show a significantly decreased trend. Therefore, the addition of catalyst in ozonation process can significantly improve the decomposition of saturated alkanes (20-30 ppm) and carboxyl/carbonyl carbons (163-190 ppm) functional groups based upon the ^{13}C NMR spectra.

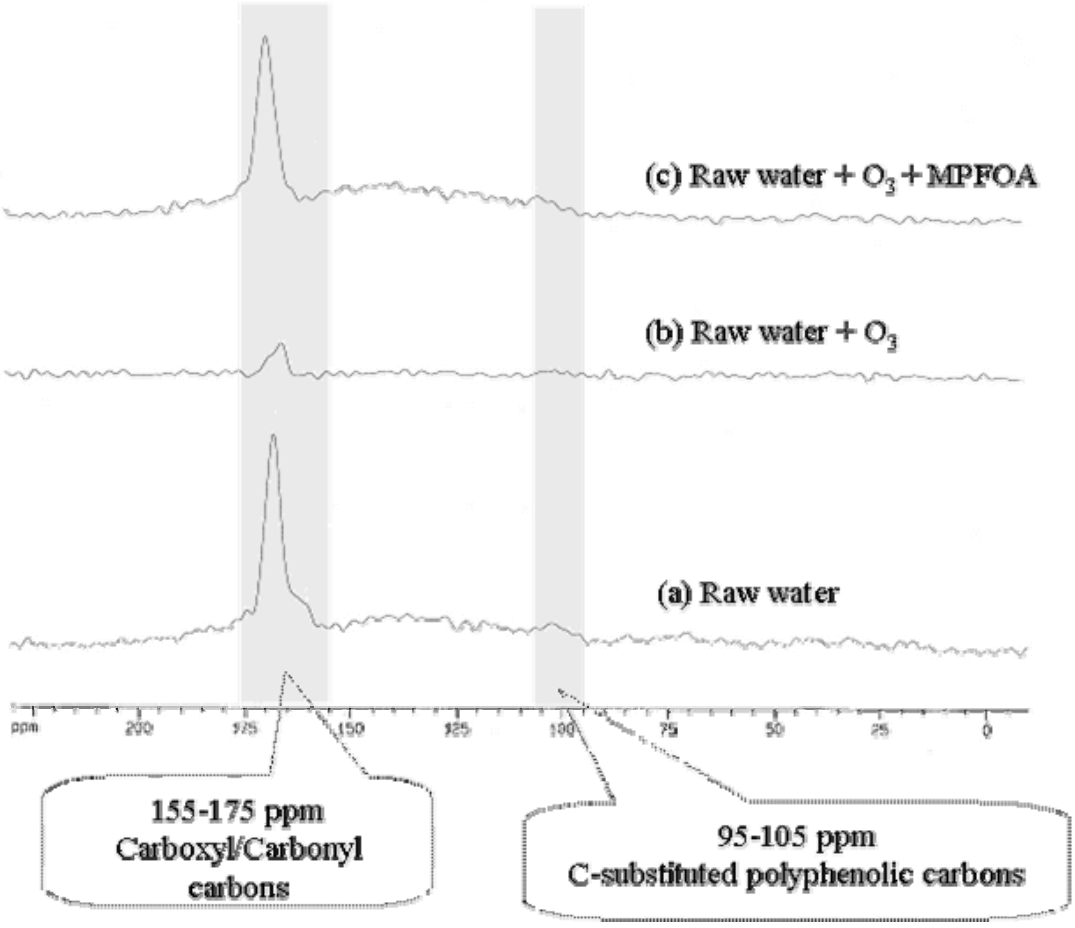

Figure 4.13 ^{13}C NMR spectra of Te-Chi Reservoir raw water (a) before ozonation (Raw water), (b) after ozonation (Raw water + O_3) and (c) after ozonation with MPFOA (Raw water + O_3 + MPFOA).

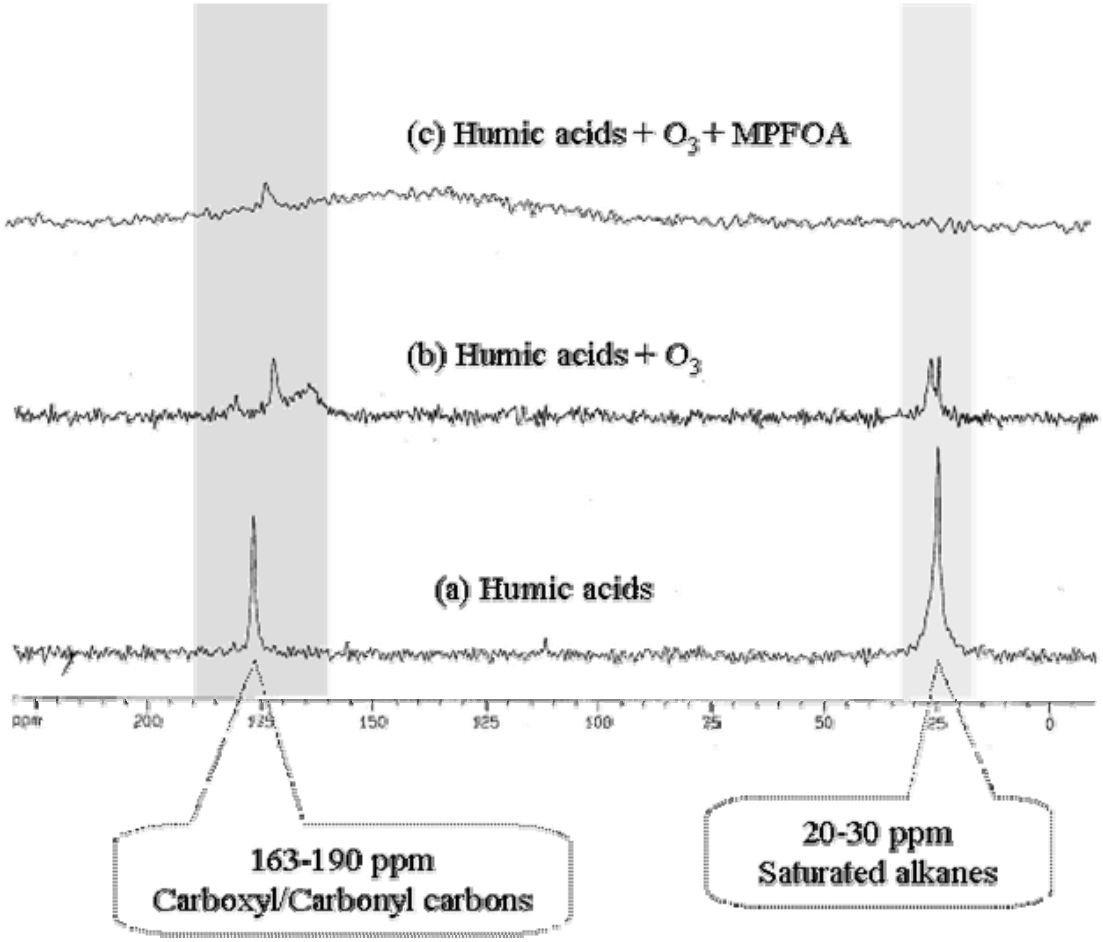

Figure 4.14 ^{13}C NMR spectra of humic acid from Te-Chi Reservoir raw water (a) before ozonation (Humic acids), (b) after ozonation (Humic acids + O_3) and (c) after ozonation with MPFOA (Humic acids + O_3 + MPFOA).

Chapter 5 Conclusions and Suggestions

5.1 Conclusions

1. The composition of NOMs is extracted and separated to five species by using XAD-8 resins as an absorbent. The percentage of HAs, FAs, hydrophobic neutrals, hydrophobic bases and hydrophilic fractions are 29.5 %, 19.5 %, 37.9 %, 2.9 % and 10.2 %, respectively.
2. The characteristics of MPFOA are determined by using of SEM/EDS, SQUID, XRD and FTIR. The analytical results confirm the formation of identify the preparation of MPFOA with superparamagnetism. The synthetic catalyst can be recovered after ozonation in the yields between 85-95 %. The recovery catalyst maintains its fractional groups identity even after 5 times of recycling by using a strong magnet.
3. The magnetic catalyst can be applied to ozonation to raise the reactivity and stability of ozone for oxidation.
4. The monitored data (ORP, DO_3, pH, OH radicals and A_{254}) can be used to develop several modified Nernst type models for the ozonation and catalytic ozonation. The on-line monitor system and modified Nernst model can provide useful information in the

process control of water treatment process.

5. The spectra of FTIR and ^{13}C NMR indicate the change of functional groups during both the ozonation and the catalytic ozonation processes. The addition of catalyst in ozonation process can significantly improve the decomposition of saturated alkanes (20-30 ppm) and carboxyl/carbonyl carbons (163-190 ppm) functional groups based upon the ^{13}C NMR spectral analytic.

5.2 Suggestions

The future investigation of this topic includes the following items:

1. To use different kinds of scavenger and compare the result with coumarin and find the possible different reaction mechanisms in the proposed system.
2. To investigate the unknown functional groups occurred in ^{13}C NMR peaks and identify their characteristics.

References

Alsheyab, M. A. and Muñoz, A. H., (2007), "Comparative study of ozone and MnO_2/O_3 effects on the elimination of TOC and COD of raw water at the Valmayor station", Desalination, 207(1-3): 179-183.

APHA, AWWA and WEF (2005), Standard methods for examination of water and wastewater, 21st Edition. American Public Health Association, Washington D. C., USA.

Barrow, G. M., (1988), Physical Chemistry, McGraw-Hill, New York.

Beltrán, F. J., Rivas, F. J. and Montero-de-Espinosa, R., (2005), "Iron type catalysts for the ozonation of oxalic acid in water", Wat. Res., 39(15): 3553-3564.

Bishop, E., (1972). Indicators. Pergamon Press, Oxford.

Bose, P. and Reckhow, D. A., (2007), "The effect of ozonation on natural organic matter removal by alum coagulation", Wat. Res., 41(7): 1516-1524.

Chang, C. N., Ma, Y. S., Fang, G. C., Chao, A. C., Tsai, M. C. and Sung, H. F., (2004), "Decolorizing of lignin wastewater using the photochemical UV TiO_2 process", Chemosphere, 56(10): 1011-1017.

Chang, F. C., Jen, J. F. and Tsai, T. H., (2002), "Hydroxyl radical in living systems and its separation methods", Chromatography B, 781(1-2): 481-496.

Charvin, P., Abanades, S., Flamant, G. and Lemort, F., (2007), "Two-step water splitting thermochemical cycle based on iron oxide redox pair for solar hydrogen production", Energy, 32(7): 1124-1133.

Chien, Y. C., Wang, H. P., Lin, K. S., Huang, Y. J. and Yang, Y. W., (2000), "Fate of bromine in pyrolysis of printed circuit board wastes", Chemosphere, 40(4): 383-387.

Chow, A. T., (2006), “Disinfection by product reactivity of aquatic humic substances derived from soils”, Wat. Res., 40(7): 1426-1430.

Chu, W., Chan, K. H. and Graham, N.J.D., (2006), “Enhancement of ozone oxidation and its associated processes in the presence of surfactant: Degradation of atrazine”, Chemosphere, 64(6): 931-936.

Deng, Y. H., Wang, C. C., Hu, J. H., Yang, W. L. and Fu, S. K., (2005), “Investigation of formation of silica-coated magnetite nanoparticles via sol-gel approach”, Colloids and Surfaces A: Physicochem. Eng. Aspects, 262(1-3): 87-93.

DeLapp, R. C., LeBoeuf, E. J., Chen, J. and Gu, B., (2005), “Advance thermal characterization of fractionated natural organic matter”, Journal of Environmental Quality, 34(3): 842-853.

Ehrman, S. H. and Friedlander, S. K., (1999), “Phase segregation in binary SiO_2/TiO_2 and SiO_2/Fe_3O_4 nanoparticle aerosols formed in a premixed flame, J. Mater. Res., 14: 4551-4561.

Hafidi, M., Amir, S. and Reve, J. C., (2005), “Structural characterization of olive mill waster-water after aerobic digestion using element”, Process Biochemistry, 40(8): 2615-2622.

Hancock, J. T., Desikan, R., Meill, S. J. and Cross, A. R., (2004), “New equations for redox and nano-signal transduction”, Journal of Theoretical Biology, 226(1): 65-68.

Hoigné, J. and Bader, H., (1976), “The role of hydroxyl radical reactions in ozonation processes in aqueous solutions”, Wat. Res., 10(5): 377-386.

Hoigné, J. and Bader, H., (1983), “Rate constants of reactions of ozone with organic and inorganic compounds in water-Π. Dissociation organic compounds”, Wat. Res., 17(2): 185-194.

Huang, W. J., Fang, G. C. and Wang, C. C., (2005), “The determination and fate of disinfection by-products from ozonation of polluted raw water”, Science of the Total Environment, 345(1-3): 261-272.

Jen, J. F., Leu, M. F. and Yang, T. C., (1998), "Determination of hydroxyl radicals in an advanced oxidation process with salicylic acid trapping and liquid chromatography", Chromatography A, 796(1): 283-288.

Kanokkantapong, V., Marhaba, T. F., Pavasant, P. and Panyapinyophol, B., (2006), "Characterization of haloacetic acid precursors in source water", Environmental Management, 80(3): 214-221.

Karnik, B.S., Davies, S.H., Baumann, M.J. and Masten, S.J., (2005), "The effects of combined ozonation and filtration on disinfection by-product formation", Wat. Res., 39(13): 2839-2850.

Kasprzyk-Hordern, B., Ziolek, M. and Nawrocki, J., (2003), "Catalytic ozonation and methods of enhancing molecular ozone reactions in water treatment", Appl. Catal. B: Environ., 46(3): 639-669.

Kasprzyk-Hordern, B., Da˛browska, A., Świetlik, J. and Nawrocki, J., (2004), "The application of the perfluorinated bonded alumina phase for natural organic matter catalytic ozonation", Engi. and Sci., 3(1): 41-50.

Kim, H. C. and Yu, M. J., (2005), "Characterization of natural organic matter in conventional water treatment processes for selection of treatment processes focused on DBPs control", Wat. Res., 39(19): 4779-4789.

Kim, H. C. and Yu, M. J., (2007), "Characterization of aquatic humic substances to DBPs formation in advanced treatment processes for conventionally treated water", Hazardous Materials, 143(1-2): 486-493.

Kitis, M., Karanfil, T., Wigton, A. and Kilduff, J. E., (2002), "Probing reactivity of dissolved organic matter for disinfection by-product formation using XAD-8 resins adsorption and ultrafiltration fractionation", Wat. Res., 36(15): 3834-3848.

Koshino, H., Satoh, H., Yamada, T. and Esumi, Y., (2006), "Structural revision of peribysins C and D", Tetrahedron Letters, 47(27): 4623-4626.

Kusic, H., Koprivanac, N. and Loncaric Bozic, A., (2006), "Minimization of organic pollutant content in aqueous solution by means of AOPs: UV- and ozone-based technologies", Chem. Engi. J., 123(3): 127-137.

Leenheer, J. A., (1981), "Comprehensive approach to preparative isolation and fractionation of dissolved organic carbon from natural waters and wastewaters", Environ. Sci. Technol., 15(5): 578-587.

Liao, C. H., Chen, W. M. and Xiao, X. M., (2007), "The generation and inactivation mechanism of oxidation-reduction potential of electrolyzed oxidizing water", J. Food Engi., 78(4): 1326-1332.

Lin, C. F., Liu, S. H. and Hao, O. J., (2001), "Effect of functional groups of humic substances on up performance", Wat. Res., 35(10): 2395-2402.

Louit, G., Foley, S., Cabillic, J., Coffigny, H., Taran, F., Valleix, A., Renault, J. P. and Pin, S., (2005), "The reaction of coumarin with the OH radical revisited: hydroxylation product analysis determined by fluorescence and chromatography", Radiation Phy. and Chem., 72(2-3): 119-124.

Lou, M. Y., Wang, D. P., Huang, W. H., Chen, D. and Liu, B., (2006), "Effect of silane-coupling agents on synthesis and character of core-shell SiO_2 magnetic microspheres", Magnetism and Magnetic Materials, 305(1): 83-90.

Lu, Y., Yin, Y., Mayers, B. T. and Xia, Y., (2002), "Modifying the Surface Properties of Superparamagnetic Iron Oxide Nanoparticles through A Sol-Gel Approach", Nano letters, 2(3): 183-186.

Ma, J., Sui, M., Zhang, T. and Guan, C., (2005), "Effect of pH on MnOx/GAC catalyzed ozonation for degradation of nitrobenzene", Wat. Res., 39(5): 779-786.

Ma, Z., Guan, Y. and Liu, H., (2006), "Superparamagnetic silica nanoparticles with immobilized metal affinity ligands for protein adsorption", Magnetism and Magnetic Materials, 301(1-3): 469-477.

Malato, S., Blanco, J., Alarcón, D. C., Maldonado, M. I., Fernández-Ibáñez, P. and Gernjak, W., (2007), "Photocatalytic decontamination and disinfection of water with solar collectors", Catalysis Today, 122(1-2): 137-149.

Meunier,L., Canonica, S. and von Gunten, U., (2006), "Implications of sequential use of UV and ozone for drinking water quality", Wat. Res., 40(9): 1864-1876.

Monteagudo, J. M., Carmona, M. and Dura'n, A., (2005), "Photo-Fenton-assisted ozonation of p-Coumaric acid in aqueous solution", Chemosphere, 60(8): 1103-1110.

Newton, G. L. and Milligan, J. R., (2006), "Fluorescence detection of hydroxyl radicals", Radiation Phy. Chem., 75(4): 473-478.

Ni, C. H., Chen, J. N., and Yang, P. Y., (2003), "Catalytic ozonation of 2-dichlorophenol by metallic ions", Water Sci. Techn., 47(1): 77-82.

Nicoli, M. C., Toniolo, R. and Anese, M., (2004), "Relationship between redox potential and chain-breaking activity of model systems and foods", Food Chem., 88(1): 79-83.

Nitin A L, N., LaConte A O, E. W., Zurkiya, A. X. and Bao, H. G., (2004), "Functionalization and peptide-based delivery of magnetic nanoparticles as an intracellular MRI contrast agent", J. Biol. Inorg. Chem., 9(6): 706-712.

Park, S. and Yoon, T., (2007), "The effects of iron species and mineral particles on advanced oxidation processes for the removal of humic acids", Desalination, 208(1-3): 181-191.

Peng, Z.G., Hidajat, K. and Uddin, M.S., (2004), "Adsorption of bovine serum albumin on nanosized magnetic particles", Journal of Colloid and Interface Science, 271(2): 277-283.

Philipse, A. P., van Bruggen, Michel P. B. and Pathmamanoharan, C., (1994), "Magnetic Silica Dispersions: Preparation and Stability of

Surface-Modified Silica Particles with a Magnetic Core", Langmuir,10(1): 92-99.

Pi, Y., Schumacher, J. and Jekel, M., (2005), "Decomposition of aqueous ozone in the presence of aromatic organic solutes", Wat. Res., 39(1): 83-88.

Prado, J., Arantegui, J., Chamarro, E. and Esplugas, S., (1994), "Degradation of 2,4-D by ozone and light", Ozone Sci. Eng., 16(3): 235-245.

Qu, J., Li, H., Liu, H., and He, H., (2004), "Ozonation of alachlor catalyzed by Cu/Al_2O_3", Catalysis Today, 90(3-4): 291-296.

Qu, X., Zheng, J. and Zhang, Y., (2007), "Catalytic ozonation of phenolic wastewater with activated carbon fiber in a fluid bed reactor", Journal of Colloid and Interface Science, 309(1): 429-434.

Rudge, S. R., Kurtz, T. L., Vessely, C. R., Catterall, L.G. and Williamson, D.L., (2000), "Preparation, characterization, and performance of magnetic iron-carbon composite microparticles for chemotherapy", Biomaterials, 21(14): 1411-1420.

Sarma, L., Devasagayam, T. P., Mohan, H., Mittal, J. P. and Kesavan, P. C., (1996), "Mechanisms of protection by buthionine sulphoximine against γ-ray-induced micronuclei in polychromatic erythrovcytes of mouse bone marrow", Int. J. Radiat. Biol., 69(5): 633-643.

Sánchez-Polo, M., von Gunten, U. and Rivera-Utrill, J., (2005), "Efficiency of activated carbon to transform ozone into ·OH radicals: Influence of operational parameters", Wat. Res., 39(14): 3189-3198.

Satoh, H., Koshino, H., Uno, T., Koichi, S., Iwata, S. and Nakata, T., (2005), "Effective consideration of ring structures in CAST/CNMR for highly accurate ^{13}C NMR chemical shift prediction", Tetrahedron, 61(31):7431-7437.

Schrank, S. G., Ribeiro dos Santos, J. N., Souza, D. S., Santos Souza, E.

E., (2007), “Decolourisation effects of Vat Green 01 textile dye and textile wastewater using H_2O_2/UV process”, Photochemistry and Photobiology A: Chemistry, 186(2-3): 125-129.

Shen, L., Laibinis, P. E. and Alan Hatton, T., (1999), “Aqueous magnetic fluids stabilized by surfactant bilayers”, Magnetism and Magnetic Materials, 194(1-3) 37-44.

Stöber, W. and Fink, A., (1968), “Controlled growth of monodisperse silica spheres in the micron size range”, Journal of Colloid and Interface Science, 26(1): 62-69.

Sun, Y., Duan, L., Guo, Z., Mu, Y. D., Ma, M., Xu, L., Zhang, Y. and Gu, N., (2005), “An improved way to prepare superparamagnetic magnetite-silica core-shell nanoparticles for possoble biological application”, Journal of Magnetism and Magnetic Materials, 285(1-2): 65-70.

Thurman, E. M. and Malcolm, R. L., (1981), “Preparative isolation of aquatic humic substances”, Environ. Sci. Technol., 15(4): 463-466.

Toor, R. and Mohseni, M., (2007), “UV-H_2O_2 based AOP and its integration with biological activated carbon treatment for DBP reduction in drinking water”, Chemosphere, 66(11): 2087-2095.

Von Gunten, U., (2003), “Ozonation of drinking water: Part I. Oxidation kinetics and product formation”, Wat. Res., 37(7): 1443-1467.

Weber, W. J., (1972), “Physicochemical processes for water quality control”, John Wiley & Sons, New York.

Wieserman, L. F., Cross, K., and Martin, E. S., (1991), U.S. Patent 4, 983, 566.

Wiles, K. B., de Diego, C.M., de Abajo, J. and McGrath, J. E., (2007), “Directly copolymerized partially fluorinated disulfonated poly(arylene ether sulfone) random copolymers for PEM fuel cell systems: Synthesis, fabrication and characterization of membranes and membrane-electrode assemblies for fuel cell applications”, Journal of

Membrane Science, 294(1-2): 22-29.

Wojnárovits, L., Pálfi, T., Takács, E. and Emmi, S. S., (2005), "Reactivity differences of hydroxyl radicals and hydrated electrons in destructing azo dyes", Radiation Physics and Chemistry, 74(3-4): 239-246.

辛汎峰，(1999)，"以臭氧及膜濾法降低優氧化水體中同有機成分生成消毒副產物潛能之探討"，東海大學環境科學系碩士班碩士論文。

吳家興，(2000)，"台灣地區水庫水源特性分及消毒副產物生成潛能之探討"，東海大學環境科學碩士班碩士論文。

陳峙霖，(2001)，"以預臭氧對腐植酸生成消毒副產物特性之探討"，東海大學環境科學研究所碩士論文。

蔡美純，(2002)，"從水中天然有機物官能基變化探討前臭氧/粒狀活性碳反應機制"，東海大學環境科學研究所碩士論文。

宋曉帆，(2003)，"利用高級處理程序及高速擷取設備輔助監測水體中天然有機物官能基特性變化及降低消毒副產物生成潛能探討"，東海大學環境科學研究所碩士論文。

梁永瑩，(2004)，"Applying Oscilloscope to Investigate the Direct and Indirect Ozone Reactions"，東海大學環境科學研究所碩士論文。

江彥霈，(2005)，“The Investigation of Two-stage Ozone Reaction in Eutrophication Reservoir Water”，東海大學環境科學研究所碩士論文。

洪詩涵，(2006)，“The investigation of free radicals on ozonation”，東海大學環境科學研究所碩士論文。

Appendix I.

The oxidized indicator reacts with a reductant, the absorbance decreases and the "reducing power" of the sample can be estimated. The redox reaction is described by

$$Oxi + ne^{-} \rightarrow \mathrm{Red} \qquad E^{0} \qquad \text{.....Eq. 1}$$

Where Oxi is the oxidized form, Red is the reduced form and n is the number of electrons transferred (Bishop, 1972). The redox potential for an indicator (E) is determined by the relative concentration (activities) of the oxidized and reduced species and the Nernst equation,

$$E = E_0 - \frac{RT}{nF} \ln\left(\frac{[\mathrm{Red}]}{[Oxi]}\right) \qquad \text{.....Eq. 2}$$

Where, E = the electrode potential of chemical reactions (mV)

E_0 = the standard electron potential (mV)

R = gas constant (8.314 V-coulombs K^{-1} mol^{-1})

T = the absolute temperature (K)

n = the number of electrochemical gram equivalent per gram mole exchanged during the redox reaction (equivalent mol^{-1})

F = Frarday's constant (96,500 coulombs equivalent^{-1})

[*Oxi*] = concentration of oxidizing agent

[*Red*] = concentration of reducing agent

Nernst equation is used for general redox reaction. A general redox reaction can be represented as Eq. 3 (Barrow, 1988):

$$aA+bB \leftrightarrow cC+dD \quad \text{.....} Eq.\ 3$$

Where *A* and *B* are reactants; *C* and *D* are products; and *a-d* are the stoichiometric coefficients for species A-D, respectively. The Nernst equation for a generalized oxidation-reduction reaction is obtained:

$$E = E^0 - \frac{RT}{nF}\ln\frac{(a_C)^c(a_D)^d}{(a_A)^a(a_B)^b} \quad or \quad E = E^0 + \frac{RT}{nF}\ln\frac{(a_A)^a(a_B)^b}{(a_C)^c(a_D)^d} \text{.....} Eq.\ 4$$

Application for ozone reaction, the main redox reaction is organic compounds convert to CO_2 and H_2O. Nernst equation can also adapt to simulate the ozonation process. The chemical redox reaction is assumed by the following generic stoichiometric shown as Eq. 5:

$$5C_xH_yO_z + O_3 + (40x+10y-20z-12)\cdot OH \rightarrow 5xCO_2 + (10x+5y-5z-3)H_2O + (20x+5y-10z-6)OH^- \text{.....} Eq.\ 5$$

Applying the standard Nernst equation in the ozone system, the

Nernst equation for the ozonation process is

$$E = E^0 + \frac{RT}{nF}\ln\left(\frac{\left[C_xH_yO_z\right]^5\left[O_3\right]\left[\cdot OH\right]^{(40x+10y-20z-12)}}{\left[CO_2\right]^{5x}\left[OH^-\right]^{(20x+5y-10z-6)}}\right) \quad \text{.....Eq. 6}$$

$$\text{or} \quad E = E^0 - \frac{(5x)RT}{nF}\ln\left[CO_2\right] - \frac{(20x+5y-10z-6)RT}{nF}\ln\left[OH^-\right]$$
$$+\frac{5RT}{nF}\ln\left[C_xH_yO_z\right] + \frac{RT}{nF}\ln\left[O_3\right] + \frac{(40x+10y-20z-12)RT}{nF}\ln\left[\cdot OH\right] \text{.....Eq. 7}$$

Simplified formula is obtained constants a', b', c and d as defined in the following equations:

$$a' = E^0 - \frac{(5x)RT}{nF}\ln\left[CO_2\right]$$

$$b' = -\frac{(20x+5y-10z-6)RT}{nF}$$

$$c = \frac{RT}{nF}$$

$$d = \frac{(40x+10y-20z-12)RT}{nF}$$

Then Eq. 7 could be simplified as Eq. 8:

$$E = a' + b'\ln\left[OH^-\right] + c\ln\left[C_xH_yO_z\right]\left[O_3\right] + d\ln\left[\cdot OH\right] \text{.....Eq. 8}$$

Replacing 2.3026×(pH-14) for ln[OH^-] obtains Eq. 9

$$E = a + b\ pH + c\ln\left[C_xH_yO_z\right]\left[O_3\right] + d\ln\left[\cdot OH\right] \text{.....Eq. 9}$$

Where $a = a' - 32.2364$

$b = 2.3026 * b'$

Appendix Π.

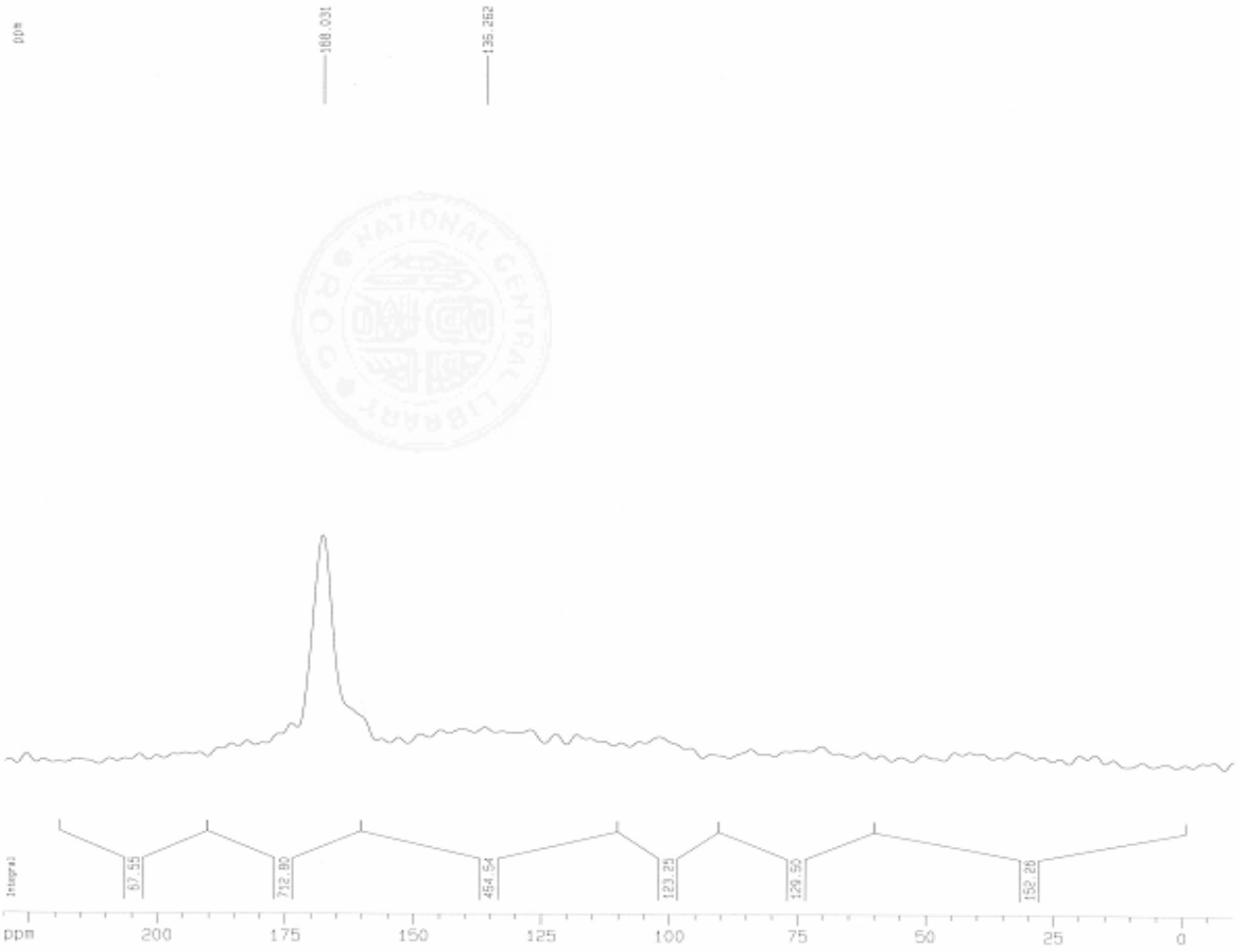


```
Current Data Parameters
NAME                  jiang
EXPNO                     1
PROCNO                    1

F2 - Acquisition Parameters
Date_              20070409
Time                  15.04
INSTRUM               spect
PROBHD    4 mm MAS 1H/BB
PULPROG          cpauto.rej
TD                     3072
SOLVENT
NS                    80000
DS                        0
SWH               41666.668 Hz
FIDRES            13.563368 Hz
AQ                0.0369140 sec
RG                    12288
DW                   12.000 usec
DE                   17.14 usec
TE                   674.9 K
D1                1.00000000 sec
D3                0.00001000 sec

======== CHANNEL f1 ========
NUC1                    13C
P15                1000.00 usec
PL1                   8.20 dB
SF01            100.4751728 MHz

======== CHANNEL f2 ========
NUC2                    1H
P3                    5.00 usec
PL2                   4.00 dB
PL12                  4.00 dB
SF02            399.5345000 MHz

F2 - Processing parameters
SI                      8192
SF              100.4626450 MHz
WDW                     EM
SSB                      0
LB                    0.00 Hz
GB                       0
PC                    1.00

1D NMR plot parameters
CX                   20.00 cm
CY                    4.30 cm
F1P                 230.000 ppm
F1                23106.41 Hz
F2P                 -10.000 ppm
F2                -1004.62 Hz
PPMCM              12.00000 ppm/cm
HZCM            1205.55176 Hz/cm
```

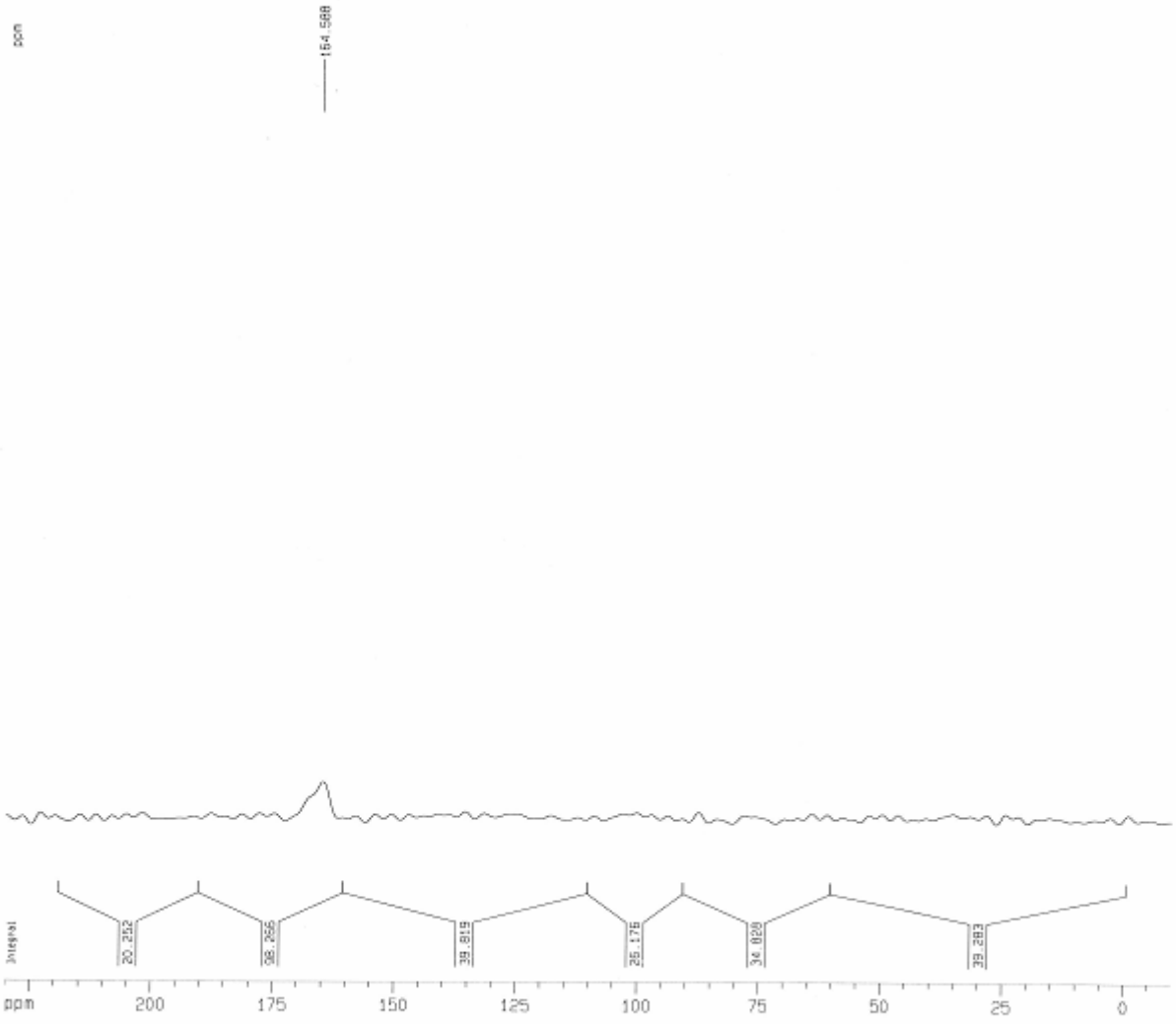


```
Current Data Parameters
NAME                  jiang
EXPNO                     2
PROCNO                    1

F2 - Acquisition Parameters
Date_              20070411
Time                  19.24
INSTRUM               spect
PROBHD   4 mm MAS 1H/BB
PULPROG           cpauto.rel
TD                     3072
SOLVENT
NS                    80000
DS                        0
SWH               41666.668 Hz
FIDRES            13.563368 Hz
AQ                0.0369140 sec
RG                     1288
DW                  12.000 usec
DE                  17.14 usec
TE                  674.8 K
D1                1.00000000 sec
D3                0.00001000 sec

======== CHANNEL f1 ========
NUC1                    13C
P15                 1000.00 usec
PL1                    8.20 dB
SF01            100.4751728 MHz

======== CHANNEL f2 ========
NUC2                    1H
P3                     5.00 usec
PL2                    4.00 dB
PL12                   4.00 dB
SF02            399.5345000 MHz

F2 - Processing parameters
SI                      8192
SF              100.4626450 MHz
WDW                     EM
SSB                        0
LB                    0.00 Hz
GB                         0
PC                      1.00

1D NMR plot parameters
CX                   20.00 cm
CY                    0.73 cm
F1P                 230.000 ppm
F1                23106.41 Hz
F2P                 -10.000 ppm
F2                -1004.62 Hz
PPMCM              12.00000 ppm/cm
HZCM             1205.55176 Hz/cm
```

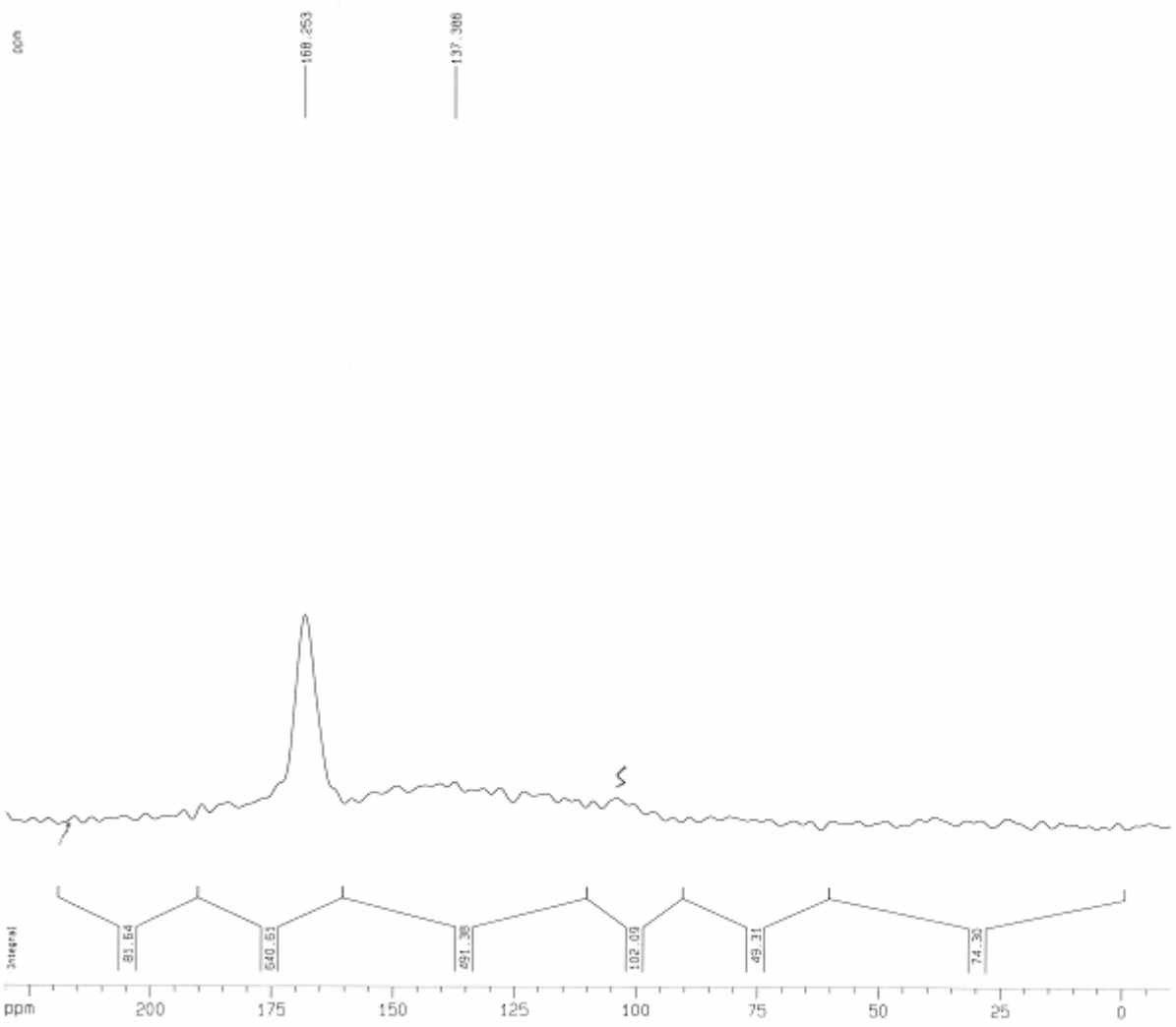

KW/O3/MPF04

rate:6500Hz

0.26379

Current Data Parameters
NAME jiang
EXPNO 5
PROCNO 1

F2 - Acquisition Parameters
Date_ 20070421
Time 15.35
INSTRUM spect
PROBHD 4 mm MAS 1H/BB
PULPROG cpauto.rel
TD 3072
SOLVENT
NS 80000
DS 0
SWH 41666.668 Hz
FIDRES 13.563368 Hz
AQ 0.0369140 sec
RG 12288
DW 12.000 usec
DE 17.14 usec
TE 675.9 K
D1 1.00000000 sec
D3 0.00001000 sec

======== CHANNEL f1 ========
NUC1 13C
P15 1000.00 usec
PL1 8.20 dB
SFO1 100.4751728 MHz

======== CHANNEL f2 ========
NUC2 1H
P3 5.00 usec
PL2 4.00 dB
PL12 4.00 dB
SFO2 399.5345000 MHz

F2 - Processing parameters
SI 8192
SF 100.4626450 MHz
WDW EM
SSB 0
LB 0.00 Hz
GB 0
PC 1.00

1D NMR plot parameters
CX 20.00 cm
CY 3.70 cm
F1P 230.000 ppm
F1 23106.41 Hz
F2P -10.000 ppm
F2 -1004.62 Hz
PPMCM 12.00000 ppm/cm
HZCM 1205.55176 Hz/cm

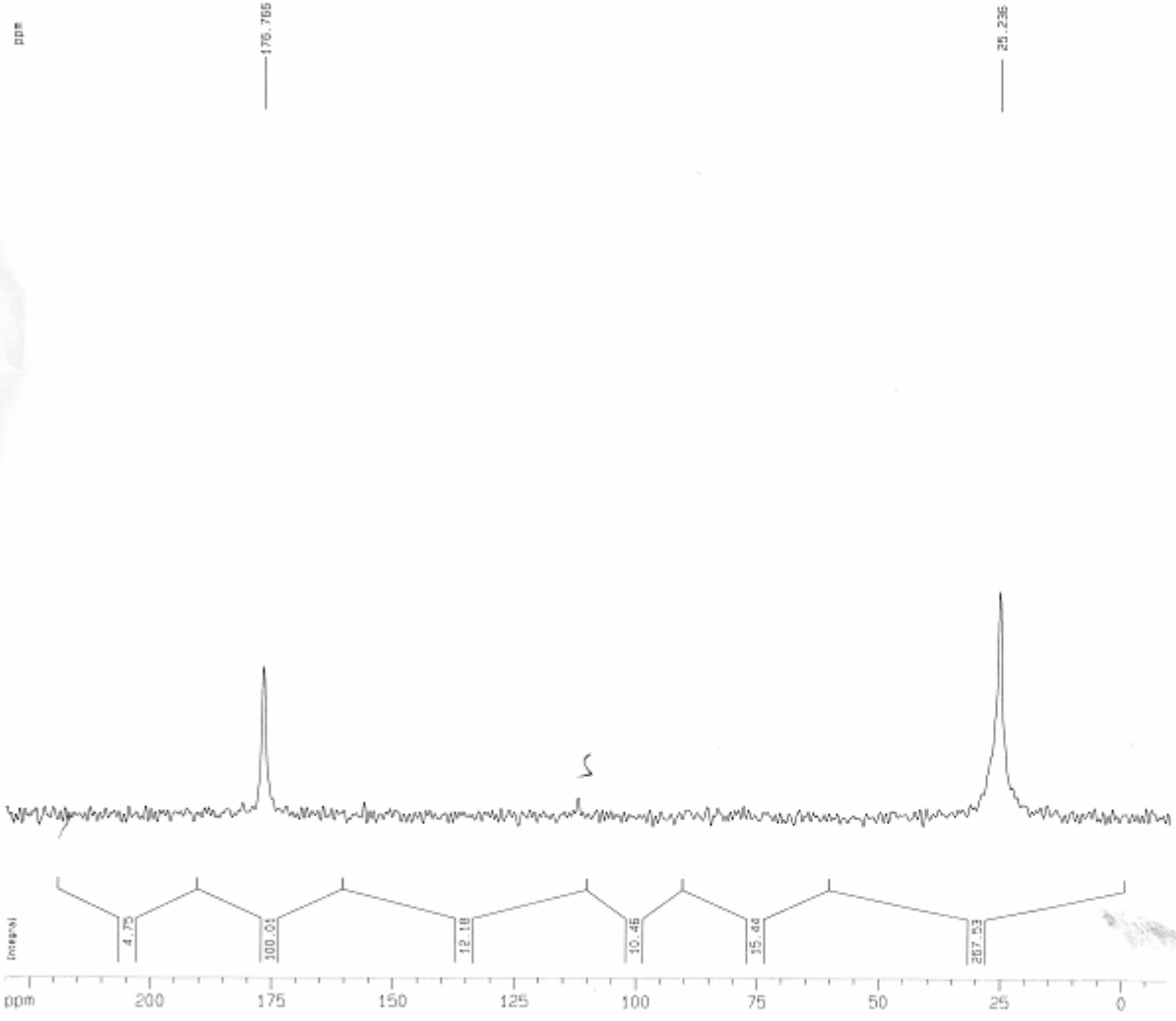

HA

Current Data Parameters
NAME jiang
EXPNO 3
PROCNO 1

F2 - Acquisition Parameters
Date_ 20070413
Time 19.16
INSTRUM spect
PROBHD 4 mm MAS 1H/BB
PULPROG cpauto.rel
TD 3072
SOLVENT
NS 80000
DS 0
SWH 41666.668 Hz
FIDRES 13.563368 Hz
AQ 0.0369140 sec
RG 12288
DW 12.000 usec
DE 17.14 usec
TE 675.4 K
D1 1.00000000 sec
D3 0.00001000 sec

======== CHANNEL f1 ========
NUC1 13C
P15 1000.00 usec
PL1 8.20 dB
SF01 100.4751728 MHz

======== CHANNEL f2 ========
NUC2 1H
P3 5.00 usec
PL2 4.00 dB
PL12 4.00 dB
SF02 399.5345000 MHz

F2 - Processing parameters
SI 8192
SF 100.4626450 MHz
WDW EM
SSB 0
LB 0.00 Hz
GB 0
PC 1.00

1D NMR plot parameters
CX 20.00 cm
CY 4.00 cm
F1P 230.000 ppm
F1 23106.41 Hz
F2P -10.000 ppm
F2 -1004.62 Hz
PPMCM 12.00000 ppm/cm
HZCM 1205.55176 Hz/cm

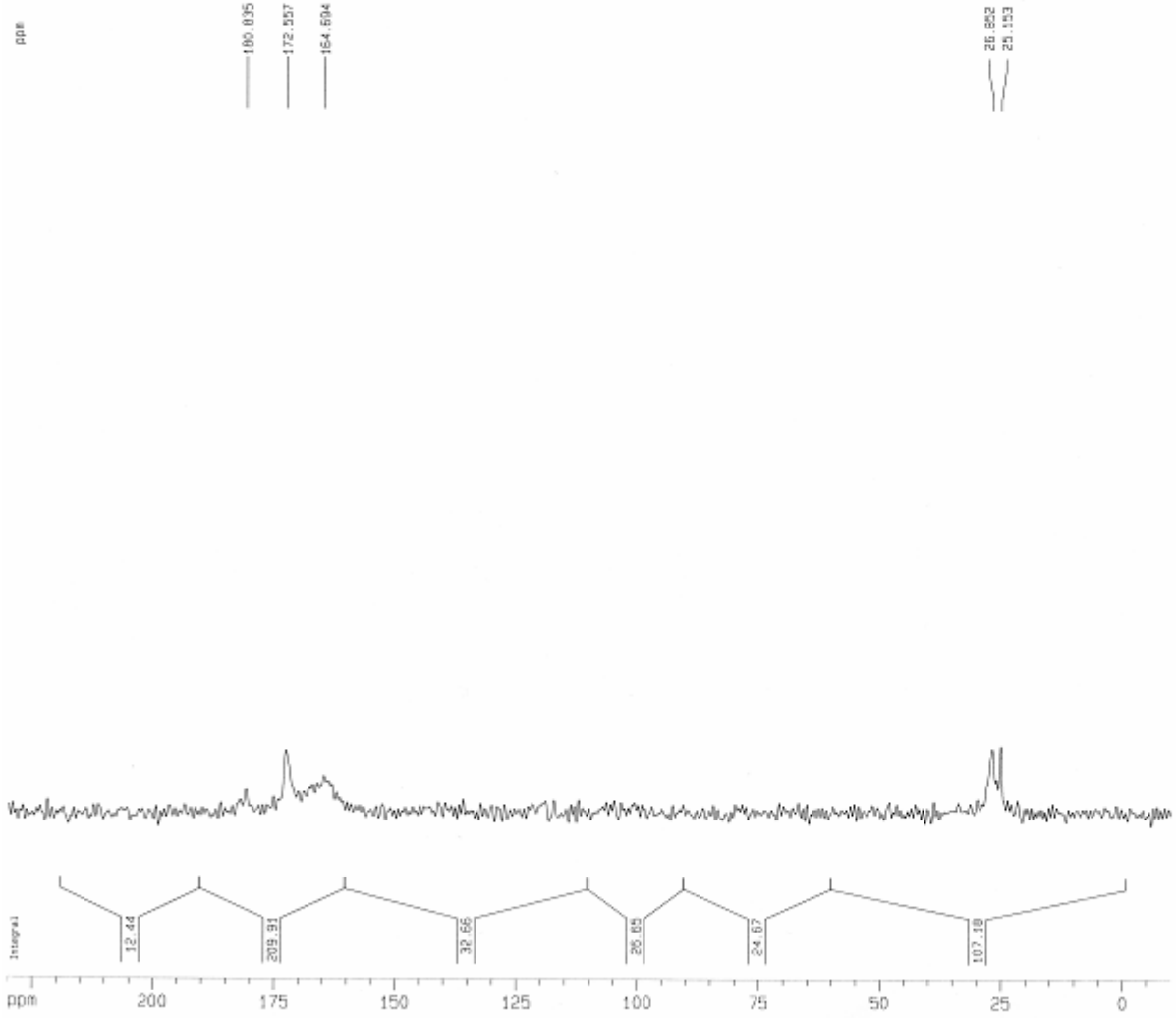


```
Current Data Parameters
NAME                  jiang
EXPNO                     4
PROCNO                    1

F2 - Acquisition Parameters
Date_              20070420
Time                  18.10
INSTRUM                spect
PROBHD    4 mm MAS 1H/BB
PULPROG          cpauto.rel
TD                     3072
SOLVENT
NS                    80000
DS                        0
SWH               41666.668 Hz
FIDRES            13.563368 Hz
AQ                0.0369140 sec
RG                    12288
DW                   12.000 usec
DE                   17.14 usec
TE                   675.9 K
D1                1.00000000 sec
D3                0.00001000 sec

======== CHANNEL f1 ========
NUC1                     13C
P15                  1000.00 usec
PL1                     8.20 dB
SFO1             100.4751728 MHz

======== CHANNEL f2 ========
NUC2                     1H
P3                      5.00 usec
PL2                     4.00 dB
PL12                    4.00 dB
SFO2             399.5345000 MHz

F2 - Processing parameters
SI                       8192
SF               100.4626450 MHz
WDW                        EM
SSB                         0
LB                       0.00 Hz
GB                          0
PC                       1.00

1D NMR plot parameters
CX                      20.00 cm
CY                       1.27 cm
F1P                    230.000 ppm
F1                   23106.41 Hz
F2P                    -10.000 ppm
F2                   -1004.62 Hz
PPMCM                 12.00000 ppm/cm
HZCM               1205.55176 Hz/cm
```

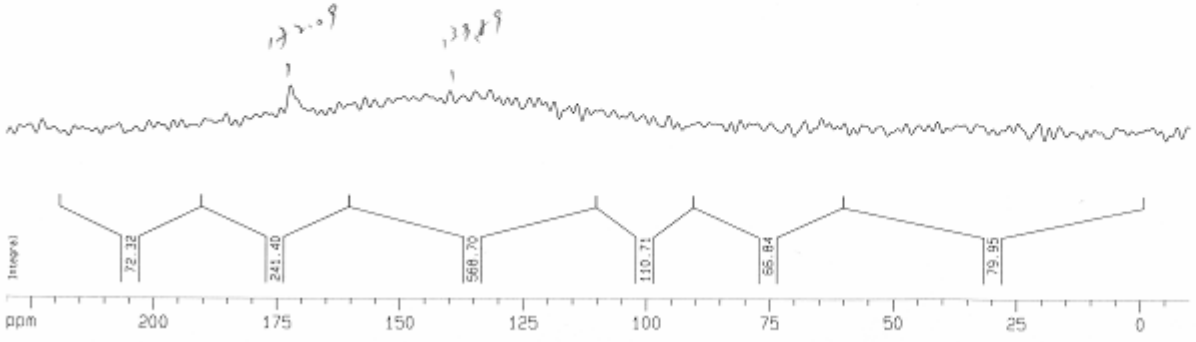


```
Current Data Parameters
NAME                  jiang
EXPNO                     6
PROCNO                    1

F2 - Acquisition Parameters
Date_              20070422
Time                 17.08
INSTRUM              spect
PROBHD    4 mm MAS tH/BB
PULPROG         cpauto.rel
TD                     3072
SOLVENT
NS                    80000
DS                        0
SWH               41666.668 Hz
FIDRES            13.563368 Hz
AQ                0.0369140 sec
RG                    12288
DW                   12.000 usec
DE                   17.14 usec
TE                   676.1 K
D1                1.00000000 sec
D3                0.00001000 sec

======== CHANNEL f1 ========
NUC1                     13C
P15                  1000.00 usec
PL1                     8.20 dB
SFO1             100.4751728 MHz

======== CHANNEL f2 ========
NUC2                     1H
P3                      5.00 usec
PL2                     4.00 dB
PL12                    4.00 dB
SFO2             399.5345000 MHz

F2 - Processing parameters
SI                       8192
SF               100.4626450 MHz
WDW                      EM
SSB                       0
LB                     0.00 Hz
GB                        0
PC                     1.00

1D NMR plot parameters
CX                    20.00 cm
CY                     0.85 cm
F1P                  230.000 ppm
F1                 23106.41 Hz
F2P                  -10.000 ppm
F2                 -1004.62 Hz
PPMCM                12.00000 ppm/cm
HZCM              1205.55176 Hz/cm
```